

**EVALUATION OF SWAT MODEL - SUBDAILY RUNOFF PREDICTION  
IN TEXAS WATERSHEDS**

A Thesis

by

**BAKKIYALAKSHMI PALANISAMY**

Submitted to the Office of Graduate Studies of  
Texas A&M University  
in partial fulfillment of the requirements for the degree of

**MASTER OF SCIENCE**

May 2006

Major Subject: Biological and Agricultural Engineering

**EVALUATION OF SWAT MODEL - SUBDAILY RUNOFF PREDICTION  
IN TEXAS WATERSHEDS**

A Thesis

by

**BAKKIYALAKSHMI PALANISAMY**

Submitted to the Office of Graduate Studies of  
Texas A&M University  
in partial fulfillment of the requirements for the degree of

**MASTER OF SCIENCE**

Approved by:

|                     |                     |
|---------------------|---------------------|
| Chair of Committee, | Raghavan Srinivasan |
| Committee Members,  | Patricia Haan       |
|                     | Bradford Wilcox     |
| Head of Department, | Gary Riskowski      |

May 2006

Major Subject: Biological and Agricultural Engineering

## ABSTRACT

Evaluation of SWAT Model: Sub-daily Runoff Prediction in

Texas Watersheds. (May 2006)

Bakkiyalakshmi Palanisamy, B.E., Tamil Nadu Agricultural University

Chair of Advisory Committee: Dr. Raghavan Srinivasan

Spatial variability of rainfall is a significant factor in hydrologic and water quality modeling. In recent years, characterizing and analyzing the effect of spatial variability of rainfall in hydrologic applications has become vital with the advent of remotely sensed precipitation estimates that have high spatial resolution. In this study, the effect of spatial variability of rainfall in hourly runoff generation was analyzed using the Soil and Water Assessment Tool (SWAT) for Big Sandy Creek and Walnut Creek Watersheds in North Central Texas. The area of the study catchments was 808 km<sup>2</sup> and 196 km<sup>2</sup> for Big Sandy Creek and Walnut Creek Watersheds respectively. Hourly rainfall measurements obtained from raingauges and weather radars were used to estimate runoff for the years 1999 to 2003. Results from the study indicated that generated runoff from SWAT showed enormous volume bias when compared against observed runoff. The magnitude of bias increased as the area of the watershed increased and the spatial variability of rainfall diminished. Regardless of high spatial variability, rainfall estimates from weather radars resulted in increased volume of simulated runoff. Therefore, weather radar estimates were corrected for various systematic, range-dependent biases using three different interpolation methods: Inverse Distance Weighting (IDW), Spline, and Thiessen polygon. Runoff simulated using these bias

adjusted radar rainfall estimates showed less volume bias compared to simulations using uncorrected radar rainfall. In addition to spatial variability of rainfall, SWAT model structures, such as overland flow, groundwater flow routing, and hourly evapotranspiration distribution, played vital roles in the accuracy of simulated runoff.

## ACKNOWLEDGMENTS

This thesis would not have been possible but for the support of one and all who have made immeasurable contributions.

I would like to first thank my advisor Dr. Raghavan Srinivasan for his immense support during all these years. He was always there for me to finish my tenure as a student. I would like to thank my committee members Dr. Patricia Haan and Dr. Bradford Wilcox for their suggestions and advice throughout this study.

Also, I would like to express my gratitude to Dr. Jeffrey G. Arnold for guiding me in SWAT model and I would like to thank Nancy B. Sammons in getting SWAT2003 version related inputs and source codes. I thank Dr. Roger Glick without whom I would not be able to complete this thesis manuscript. And I thank Mr. Kurt Reitsma for his valuable advice and hydrology related information during the final stage of my thesis.

I also want to thank Sonya Stranges for helping me with finishing all the paper work related to my thesis and defense while I was out of town. I thank all my friends and everybody who have contributed directly or indirectly to this study and the preparation of this manuscript.

And finally I thank God for blessing me to work with these great people on this great project.

## TABLE OF CONTENTS

|  | Page |
|--|------|
| ABSTRACT .....   | iii  |
| ACKNOWLEDGMENTS.....   | v    |
| TABLE OF CONTENTS .....  | vi   |
| LIST OF TABLES .....   | viii |
| LIST OF FIGURES.....   | ix   |
| <br>CHAPTER  |      |
| I    INTRODUCTION.....   | 1    |
| II   REVIEW OF LITERATURE .....  | 5    |
| Effect of spatial variability of rainfall in hydrologic<br>and water quality modeling..... | 5    |
| Differences between point and spatially distributed<br>rainfall measurements.....          | 7    |
| Hydrologic modeling using spatially distributed<br>rainfall.....                           | 11   |
| III  MATERIALS AND METHODS .....   | 15   |
| Description of the study area.....   | 15   |
| Soils of the study area .....  | 16   |
| Landuse and topography .....   | 17   |
| Model description and setup .....  | 18   |
| Weather data collection.....   | 19   |
| Data processing .....  | 20   |
| Comparison statistics.....   | 23   |
| IV  RESULTS AND DISCUSSION .....   | 28   |
| Selection of optimal radar rainfall estimating method                                      | 28   |
| Seasonal comparison of raingauge and optimal<br>radar rainfall measurements.....           | 31   |
| Conditional analysis of rainfall with respect to zero...                                   | 33   |
| Comparison of uncorrected and bias adjusted optimal  |      |

| CHAPTER  | Page |
|--|------|
| radar rainfall measurements .....  | 36   |
| Comparison of simulated runoff using five<br>different rainfall inputs ..... | 38   |
| Sensitivity analysis .....   | 59   |
| IV CONCLUSION.....   | 61   |
| REFERENCES.....  | 64   |
| VITA.....  | 70   |

## LIST OF TABLES

| TABLE |  | Page |
|-------|--|------|
| 1     | Monthly rainfall analysis between gauge and uncorrected, bias adjusted optimal radar estimates for the year 2002 for Big Sandy Creek Watershed ..... | 39   |
| 2     | Monthly rainfall analysis between gauge and uncorrected, bias adjusted optimal radar estimates for the year 2002 for Walnut Creek Watershed.....     | 40   |
| 3a    | Maximum rainfall observed from various rainfall sources for selected runoff producing events for Big Sandy Creek Watershed                           | 41   |
| 3b    | Rainfall distribution of the selected runoff producing events for Big Sandy Creek Watershed.....   | 42   |
| 4a    | Maximum rainfall observed from various rainfall sources for selected events for Walnut Creek Watershed.....  | 43   |
| 4b    | Rainfall distribution of the selected runoff producing events for Walnut Creek Watershed.....  | 43   |
| 5     | Statistics used for comparing observed and simulated streamflow for Big Sandy Creek Watershed.....   | 52   |
| 6     | Statistics used for comparing observed and simulated streamflow for Walnut Creek Watershed.....  | 53   |
| 7     | Parameter range of variables derived from Sensitivity analysis.....  | 60   |



## LIST OF FIGURES

| FIGURE   | Page |
|--|------|
| 1      Big Sandy Creek and Walnut Creek watersheds, raingauges,<br>radar gauges and waste water treatment plants .....   | 17   |
| 2      Regression of radar rainfall estimates derived using <i>at-gauge-location</i><br>and <i>9-cell minimum difference</i> method for raingauge Fortworth<br>for the year 2003.....  | 29   |
| 3      Regression of radar rainfall estimates derived using <i>at-gauge-location</i><br>and <i>9-cell minimum difference</i> method for raingauge Springtown<br>for the year 2003..... | 30   |
| 4      Seasonal comparison of raingauge and optimal radar rainfall estimates<br>for the year 2003.....   | 32   |
| 5      Regression of conditional optimal radar rainfall estimates with<br>rainfall measurements, with respect to zero, of raingauge<br>fortworth for the year 2003.....                | 33   |
| 6      Regression of conditional optimal radar rainfall estimates with rainfall<br>measurements, with respect to zero, from raingauge Springtown<br>for the year 2003.....             | 34   |
| 7      Seasonal comparison of conditional raingauge and optimal radar<br>rainfall estimates, with respect to zero, for the year 2002.....  | 35   |
| 8      Calibration event selected for Big Sandy Creek Watershed starting on<br>02/23/2001.....   | 45   |
| 9      Calibration event selected for Big Sandy Creek Watershed starting on<br>03/20/2002.....   | 46   |
| 10     Calibration event selected for Big Sandy Creek Watershed starting on<br>04/07/2002.....   | 47   |
| 11     Calibration event selected for Big Sandy Creek Watershed starting on<br>05/25/2002.....   | 48   |
| 12     Calibration event selected for Big Sandy Creek Watershed starting on<br>06/04/2002.....   | 49   |

| FIGURE | Page  |
|--------|---|
| 13     | Calibration event selected for Walnut Creek Watershed starting on 09/11/2003..... |
|        | 50  |

## CHAPTER I

### INTRODUCTION

Streamflow, the total discharge of water within a watershed, is comprised of runoff, groundwater flow, wastewater discharge, diversions, and other sources. It forms a significant supply of water for agricultural, residential, and industrial use, as well as power generation and other purposes such as recreation and wildlife habitat. The amount of streamflow received at the outlet of the watershed will be affected by various environmental factors such as rainfall, soil type, land use and land cover, and other input sources, such as water discharged from wastewater treatment plants. Among these variables, rainfall is considered to be the key input since it drives the hydrologic cycle. Apart from its significance in the hydrologic cycle, great variability exists in rainfall across space; a classic example is that in Arica, Chile the annual average rainfall is 0.5 mm while in comparison Mount Waialeale, Hawaii receives 11,680 mm per year on average (Chow et al., 1988).

When rainfall is measured using the traditional raingauge method, the spatial variability cannot be captured by each raingauge. Thus, raingauge measurements are considered to give a poor representation of areal precipitation, specifically in large watersheds with sparse networks (Neary, et al., 2004). To address the issue of spatial variability, raingauges have been replaced by weather radars, which indirectly estimate rainfall in very fine spatial resolution. Because of the ability to resolve spatial and

---

This thesis follows the style of *Hydrological Processes*.

temporal variability across a watershed that are pertinent to hydrologic applications, radar rainfall estimates are considered superior to gauge rainfall measurements, which makes them a significant input in hydrologic modeling. Hence, numerous studies have used weather radar rainfall products to simulate runoff and flood forecasting (Zhang et al., 2004; Bedient et al., 2003; Whiteaker et al., 2006).

Even though radar rainfall has been used in a wide range of hydrologic applications, the accuracy of these hydrologic outputs is still of concern because of the bias in radar estimates (Durrans et al., 2002). Bias can arise from sources such as distance between the location of the radar and the perimeter set around that radar to estimate rainfall and the systematic difference in rainfall estimating algorithms (Smith et al., 1996). Zhang et al. (2004) commented regarding the effect of accuracy of radar rainfall in hydrologic simulation as follows:

It is not universally true that use of higher-resolution precipitation data will lead to more accurate basin outlet hydrographs; it requires further testing.

Results from a study by Johnson et al. (1999) also stated that radar-based runoff simulation resulted in some erroneous hydrographs.

Therefore, further testing of radar rainfall should be performed in order to minimize the biases and to derive optimal rainfall estimates, which in turn increase the accuracy of hydrologic simulation. This study focuses on adjusting the bias in radar rainfall and examines the effectiveness of these bias-corrected rainfall estimates in runoff simulation using Soil and Water Assessment Tool (SWAT). SWAT (Arnold et al., 1993) is a semi-distributed, physically-based hydrologic model, which mimics the actual hydrologic cycle using water balance methods. Originally, SWAT was developed as a

non-point pollution model which estimated the effects of various land management practices on water quality. As it evolved, SWAT has been used both as a hydrologic and water quality model due to its ability to accommodate a great range of inputs for very large basins over long periods of time. Numerous hydrologic and water quality studies have been performed using SWAT on daily time-steps with promising results (Jayakrishnan et al., 2004; Benaman and Shoemaker, 2005; Griensven and Bauwens, 2004; Tripathi et al., 2004; Arnold et al., 2005). Increasing awareness of natural disasters such as flooding with the advent of remote sensing technologies led the researchers to estimate runoff on a real time basis (on sub-daily, sub-hourly time-steps). A study by Jayakrishnan (2001) used the SWAT model to simulate runoff on an hourly basis using both raingauge and radar rainfall values for watersheds in Texas. Results from that study showed that hourly streamflow simulated using SWAT showed noticeable volume and phase difference when compared against observed hourly streamflow. It was concluded from that study that SWAT should be tested in order to increase its effectiveness to simulate runoff on an hourly time step using both point measured and spatially distributed radar rainfall.

Thus, in addition to an attempt to minimize uncertainty in rainfall, this research concentrated on evaluating runoff generation in shorter time-steps using SWAT. For this purpose, hourly rainfall from both raingauges and radar were used for simulating runoff for Big Sandy Creek and Walnut Creek Watersheds in the Trinity River Basin. Bias in radar rainfall values was corrected with reference to raingauge measurements. Finally, bias adjusted radar values were used to simulate runoff on an hourly basis and compared

to measured runoff values. Based on the facts explained in above section, the objectives of this study can be summarized as follows:

- 1) Evaluate the effectiveness of the SWAT model to accurately simulate runoff on a sub-daily time-step.
- 2) Evaluate the effect of spatially distributed, unadjusted, and bias adjusted radar rainfall on real time hydrologic simulation.

## CHAPTER II

### REVIEW OF LITERATURE

#### **Effect of spatial variability of rainfall in hydrologic and water quality modeling**

Rainfall varies greatly across space and time because of the range of landscapes and various climatic factors that exist. This variation in rainfall across space should be taken into consideration when modeling quantity and quality of water resources. A study by Kuczera and Williams (1992) suggests that not taking into consideration the spatial distribution of rainfall events significantly increases uncertainty in the estimation of hydrologic outputs. Syed et al. (2003) studied the relationship of spatial characteristics of thunderstorm rainfall fields to runoff in the 148 km<sup>2</sup> USDA–ARS Walnut Gulch Experimental Watershed near Tombstone, Arizona. The researchers concluded that sampling density of the raingauges plays an important role in better identifying and defining runoff-producing storm cores. Bacchi and Kottagoda (1995) recognized that the regularity of the correlation structure of rainfall relates to the number of pairs of stations used in the analysis. They showed that the raingauge density becomes a crucial point for inferring the behavior of the spatial correlation pattern.

Rainfall captured by only one gauge or a few gauges increases the bias in inputs when high-density raingauges are needed to give an adequate representation of rainfall over the watershed (Troutman, 1983). Derivation of runoff volume and sediment load caused by varying the spatial distribution of rainfall input to the Agricultural Non-Point Source (AGNPS) pollution model by Young et al. (1992) showed that total Nitrogen (N) loss was four times more, and the total Phosphorus (P) loss and sediment yields were

five times greater than the estimates obtained from using an average uniform rainfall to the model. The information from this study implies that hydrologic and water quality outputs greatly depend on the type of variation of rainfall used as input in the model. The greater the ability to characterize the spatial variability of rainfall, the less the uncertainty of the model outputs in hydrologic and water quality modeling.

A study by Chaubey et al. (1999) in quantifying models' hydrologic and water quality output uncertainty due to spatial variability of rainfall using the AGNPS model showed that bias in runoff varied in the range of  $-31$  to  $34$  mm with increasing spatial variability of rainfall; hence, it was concluded from the study that assumption of spatial homogeneity may be invalid in hydrologic and water-quality modeling.

Shah et al. (1996) and Yang et al. (1998) concluded that rainfall with coarse spatial and temporal resolutions can pose a serious problem in watershed runoff generation. Sun et al. (2002) used THALES hydrologic model to simulate runoff using point rainfall and spatially distributed rainfall for a small catchment in South Australia. The spatially distributed rainfall was derived using three different interpolation approaches, elevation-weighted, simple averaged and distance weighted. The results from this study showed that spatially distributed rainfall from all abovesaid methods enhanced the performance of runoff generation more than that of point rainfall measurement. Hence, to alleviate these possible errors introduced by spatial variability of rainfall in hydrologic and water quality modeling, inputs with very fine resolution in terms of space and time should be used for hydrologic simulations to achieve better representation of watershed processes. One such input is rainfall estimates from weather



radars. Weather radars are excellent precipitation acquisition instruments which renders rainfall at a spatial resolution of  $4\text{km}^2$ . The following section discusses the differences between spatially distributed and point measured rainfall.

### **Differences between point and spatially distributed rainfall measurements**

Limitation of sparse raingauge density imposes uncertainty in rainfall as an input, and thus leads to an inaccurate water quality and hydrologic outputs. This limitation may be overcome through the use of weather radar rainfall products. In recent years, numerous studies have been done comparing raingauge and radar data. Smith et al. (1996) compared radar and raingauge values for the Southern Plains of the United States. While analyzing the spatial coverage of heavy rainfall events, the radar performed better than even the densest raingauge network (200 raingauges). Rainfall values exceeding 25mm were observed from a radar coverage area of  $1730\text{km}^2$  while the maximum rainfall recorded by raingauges was only 22mm. Jayakrishnan et al. (2004) found that 88% of COOP raingauges of 545 stations in and around the Texas Gulf Basin underestimated daily rainfall values when compared with radar estimates for the years 1995–1999. The comparison of rainfall was performed conditionally with respect to zero with the estimation difference in the range of -57 to +60%.

Though radar estimates rainfall indirectly using a rainfall-reflectivity relationship and the accuracy of estimation varies across the globe, it resolves the issue of spatial variability imposed by point rainfall estimates (Neary et al., 2004). Joss and Lee (1995) compared two Swiss radars and a network of raingauges for an 8-year period in the Swiss Alps. They concluded that radar rainfall can be used to provide better quantitative

precipitation amounts for operational flood warnings in the Swiss Alps. Radar rainfall data in urban drainage modeling can be used in lieu of point estimates, and are considered to be a greater enhancement of point rainfall values (Einfalt et al., 2004). Also, Einfalt et al. (2004) have commented that radar rainfall data is superior to raingauge data when it comes to providing online applications and off-line analysis of high intensity events. Racy and Kopsky (1995) even noted that the radar will one day provide highly accurate precipitation estimations, which will be better than point rainfall.

In addition to studies presented in the previous section, numerous other studies have compared radar derived and raingauge measured rainfall values (Stellman et al., 2001, Johnson et al., 1999). Most of these studies compared either radar data *at-gauge-location* or *mean areal precipitation* (MAP) across the study area. However, comparing rainfall values *at-gauge-location* introduces bias in terms of deviation of raingauge location from the location of radar grid and also mapping errors in radar estimates due to the combined effects of scale and shape distortions which will vary with latitude (Reed and Maidment, 1999). Jayakrishnan (2004) showed that the percentage of first order weather stations of the National Weather Service having the total difference within  $\pm 500\text{mm}$  of rainfall increased to 63% from 40% when compared to the radar values *at-gauge-location*. A typical 8-inch raingauge samples rainfall over an area of  $0.3\text{ km}^2$ , while radar samples the average precipitation accumulation over an area of  $4\text{ km}^2$ . This huge difference in spatial variability of radar and gauge locations can impose inherent differences in precipitation estimates. Young et al. (1999) compared radar-gauge rainfall on an hourly basis. In the analysis, only nonzero rainfall was observed both from gauge

and radar which were obtained using *at-gauge-location* method. Their results showed that the radar estimates tend to be lower than the gauge measurements, especially in cold season and at longer ranges from the radar.

When comparing mean areal precipitation (MAP) estimates from gauge and radars for the Southern Plains for a period of three years, for storm events, radar was found to capture more events than the gauges did and radar underestimated rainfall by 5 to 10% (Johnson et al., 1999). Stellman et al. (2001) compared the MAP of radar data with the MAP from raingauge based data for the National Weather Service River Forecasts Centers in Culloden Basin, Georgia. They observed that the minimum difference between the two MAPs for rainfall events greater than 19.05 mm occurred during the summer. In the winter season, however, the raingauge MAP exceeded the radar MAP by 25-150%. MAP of the gauge data is calculated using interpolation techniques as simple as Thiessen polygon method or as complex as Kriging methods. Even though, these areal averaging methods are based on the distance between the gauges, unless there is a very high density of rainfall stations, it is difficult to quantify the uncertainty imposed by spatial variation of rainfall accurately. Thus, both comparing the radar data at gauge locations and comparing the MAPs of two sources will tend to introduce bias in volume of rainfall over an area regardless of its size. Another study by Stellman et al. (2001) compared MAPs derived from radar and raingauges for the headwaters of the Flint River Basin in central Georgia. They found that the MAP of radar underestimates the raingauge MAP by 38% during the winter, but showed a similar trend during the summer.

Regardless of the under- or over-estimation of radar over raingauge values, studying the effects of radar estimates in various fields was still found to be useful. Grecu and Krajewski (2000) in their study on rainfall forecasting concluded that variational assimilation of radar data in cloud models may be effective in rainfall forecasting, regardless of the uncertainty of model parameters. Grimes et al. (1999) worked on merging raingauge and satellite rainfall values by a block Kriging method to obtain optimal rainfall values over Niger, Africa. The satellite rainfall values were collected from a geostationary satellite and EPSAT (**E**stimation of **P**recipitation by **S**ATellite-Niger experiment) raingauge network of 94 gauges. The estimates from the merged satellite and raingauge estimates showed promising and improved spatial pattern of rainfall.

In addition to the radar estimation algorithm and the distance of the radar to the estimation range in radar rainfall products, bias in radar rainfall can also be introduced by the type of raingauge used to calibrate or verify the estimated rainfall product. Jayakrishnan et al. (2004) compared radar estimates against raingauge rainfall observed from First Order (FO) National Weather Service stations and also cooperative (COOP) stations that are considered as second order stations. First order stations are equipped with better instruments and trained personnel and maintained by the Federal Aviation Administration; the cooperative stations are operated by state/federal agencies, local governments, radio stations, businesses or citizens on a voluntary basis. The results from this study resulted in a coefficient of efficiency (COE) of greater than 0.5 at 71% of the FO locations while only 37% of COOP stations had a COE greater than 0.5. They also

compared average radar values from a 3x3 analysis window of radar grids and gauge measurements. The study concluded that inclusion of average radar value from the 3x3 window of radar grids decreased the COE values, when compared with the COE values calculated for the rainfall values from *at-gauge-location* method. It is, therefore, imperative that an accurate radar rainfall extraction method be used to minimize the bias between radar and gauge rainfall. In this work the *9-cell minimum difference* method was used to address the problems specified above regarding the selection method of radar rainfall. This method extracts radar rainfall within a 3x3 analysis window that shows minimum bias with the gauge measurements.

### **Hydrologic modeling using spatially distributed rainfall**

In recent years, the use of radar data in hydrologic modeling has become a popular research tool because of its ability to estimate outputs with high spatial resolution rainfall. Since the emergence of calibrated, more accurate radar data in 1995, the use of weather radar products in hydrologic modeling has become an inseparable source of input in such endeavors as runoff , flood prediction models, and characterization of extreme rainfall events. In contrast, for these same end purposes, raingauge data poses a limitation in terms of density of network. When discussing the use of radar estimates in hydrology, Krajewski and Smith (2002) concluded that radar rainfall can be used for flash-flood forecasting and water conservation design and management applications in small basins. Finnerty and Johnson (1997) used Sacramento Soil Moisture Accounting (SAC-SMA) for runoff generation with MAPs of gauge and radar rainfall. From the results they concluded that SAC-SMA model parameters were

strongly linked to spatial and temporal resolution of precipitation input, which suggests that radar data can be used in lieu of raingauge data to give potential improvements in hydrologic model outputs. Koren et al. (1999) used four different hydrological models, SAC-SMA, reformulated SAC-SMA, Oregon State University (OSU) and Simple Water Balance (SWB) model to produce runoff using different resolutions of spatially averaged radar hourly rainfall for Red River Basin at the Oklahoma-Arkansas border. The study found that spatially distributed rainfall is a primary factor of runoff reduction and rainfall variability became a major factor in runoff production from a large watershed.

Continuing the efforts of using radar rainfall in hydrologic modeling, Vieux and Bedient (1998) concluded that radar rainfall generated accurate runoff when compared against that of gauge generated runoff.

Even though radar rainfall was able to resolve the issue of variation of rainfall across space, when these values were used in hydrologic models it suggested that quality of these data should be improved in order to produce more accurate runoff hydrograph. When runoff was generated using spatially averaged and grid-distributed radar rainfall, significant bias was observed in the simulated runoff (Peters and Easton, 1996). Borga (2002) performed runoff simulation for a watershed in Southwest England with radar rainfall estimates adjusted and not adjusted for range dependent bias. The adjustment was performed by applying the bias from the radar based on point gauge measurements to the entire radar domain. The results from the study indicated that care should be taken when using unadjusted radar rainfall estimates for runoff modeling. The bias adjusted radar values showed improved performance of simulating runoff with simulation

efficiency over 0.75. In an effort to increase the effectiveness of radar rainfall in hydrologic applications, Creutin et al. (1988) employed a geostatistical approach to combine gauge and radar rainfall measurements. The Cokriging method was used for daily rainfall events that occurred in the Paris, France region. The results from that preliminary study concluded that raw radar data posed severe limitations when used in hydrologic applications while the proposed geostatistical approach showed improvement in the raw radar data. Neary et al. (2004) used radar precipitation for hydrologic simulation in two subbasins of Cumberland River Basin in Middle Tennessee. The HEC-HMS model was used generate runoff with gauge and stage III radar rainfall values. The results from that study showed the inability of radar rainfall to produce accurate runoff volume than that of gauge rainfall values at low rainfall rates. The reason for this behavior of radar rainfall was attributed to the fact that these values should be corrected for systematic bias. Todini (2001) employed a Bayesian technique for reduction of radar rainfall combining raingauge measurements on the Upper Reno River Catchment with an area of  $1051\text{km}^2$  near Bologna, Italy. Twenty-six raingauges are deployed across this catchment and the radar measurements were obtained from Regional Meteorological Service. Runoff was simulated using gauge rainfall which was interpolated using block Kriging. Results indicated that the hydrologic outputs were totally unbiased and the noise variance in the radar estimates was reduced substantially when the spatially distributed rainfall was used to generate runoff.

Hence, to address the problems discussed above with raw radar rainfall product, our research employed a bias adjustment procedure across the study area. The method of this procedure will be explained in the next section.



## **CHAPTER III**

### **MATERIALS AND METHODS**

The Big Sandy Creek and Walnut Creek watersheds in the Upper Trinity River Basin were selected for this research. Hourly runoff was simulated using SWAT with hourly rainfall measured both from raingauges and radar. In addition to raw radar estimates, bias adjusted radar rainfall was used for runoff generation. Various comparison statistics, such as Mean Absolute Error (MAE), Nash Sutcliff Efficiency (NSE), Coefficient of Determination ( $R^2$ ), Normalized Peak Error (NPE), Percentage Relative Volume Error (PRVE), Peak Timing Error (PTE), and Index of Agreement (IOA) were used to quantify the ability of SWAT to accurately simulate runoff with three different types of rainfall input data; point raingauge measurements, spatially distributed raw radar rainfall and bias adjusted radar rainfall.

#### **Description of the study area**

The Upper Trinity River Basin was selected for this study. It is located in North Central Texas, and contains all or part of Archer, Clay, Jack, Montague, Parker, Tarrant, Wise and Young counties. The Upper Trinity River Basin was divided into two sub basins: Big Sandy Creek and Walnut Creek as streamflow observations were available only at these two locations (Figure 1). The drainage area of these watersheds was 808 km<sup>2</sup> and 196 km<sup>2</sup>, respectively. On average, annual rainfall in these two watersheds range from 635 to 762 mm. About 60% of the rain falls from March through October. Average seasonal snowfall in these areas is 101.6 mm. Even though the number of days with snowfall greatly varies from year to year, the maximum one day snowfall is

25.4 mm. The average maximum winter temperature is 45°F, and the average daily minimum temperature is 31° F. Average maximum temperature in summer is 97°F. During late winter and early spring, the flow in the study area almost reaches zero. An increase in streamflow occurs during late spring and early summer when high intensity storm events are observed.

Waste water treatment plant (WWTP) operated in these watersheds (Figure 1) contribute dry weather flow. Average daily release from these WWTPs is 3,785m<sup>3</sup>, though the discharge from these plants varies based on the season, seasonal rainfall distribution and depth of flow in the channels. On average, the percentage contribution of these plants to streamflow is annually around 32%.

### **Soils of the study area**

The soil dataset for the study areas was obtained from the Soil Survey Geographic (SSURGO) database. The SSURGO database has very high spatial resolution (1:12,000 to 1:63,000) compared with the State Soil Geographic (STATSGO) database, with a scale of 1:250,000. SSURGO data thus provides detailed soil properties at county scale; while STATSGO provides soil data at statewide scale. Soil texture in these watersheds varies from very fine sandy loam at the surface to sandy clay loam at the subsurface with gentle slope. The depth of the surface layer ranges from 0.0-0.4m and the depth of the subsurface layer ranges from 0.4m to 1.5m. The bedrock lies at the depth of greater than 1.5m while the water table is located below a depth of 1.8m. The subsurface layer is underlain by soft rocks or weakened limestone in these areas.

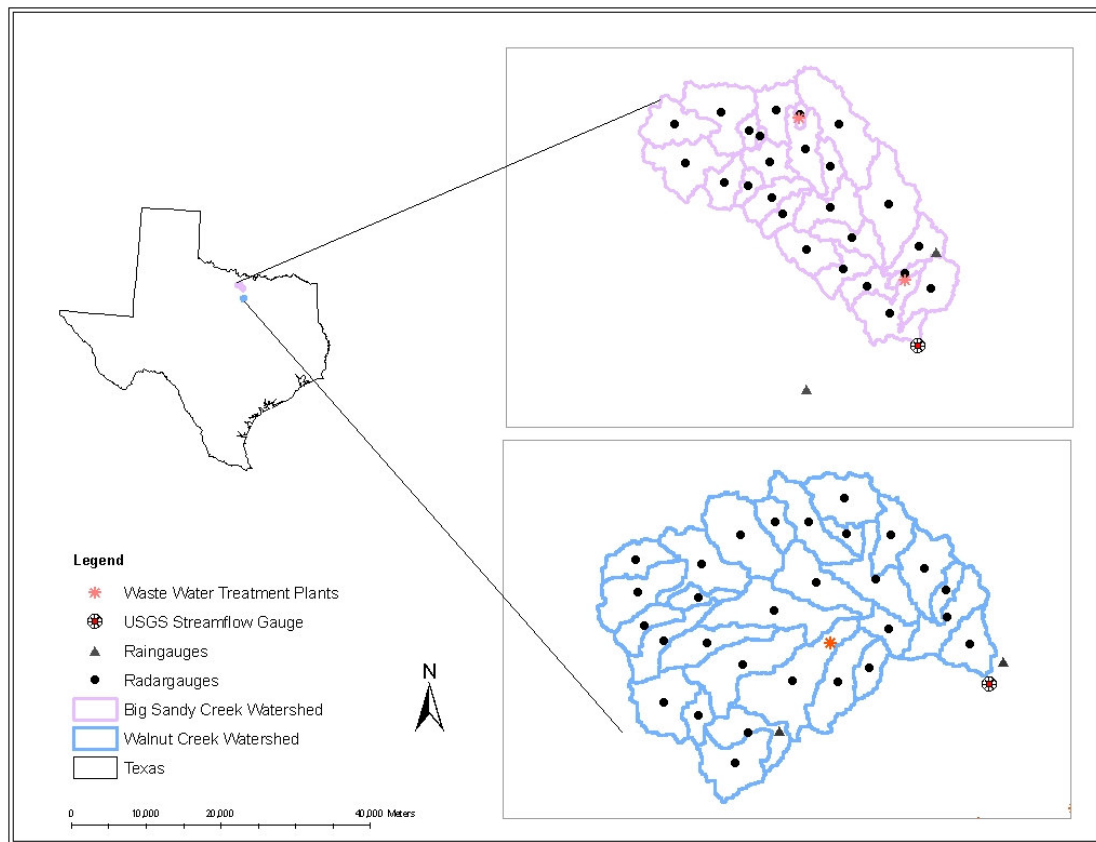


Figure 1. Big Sandy Creek and Walnut Creek watersheds, raingauges, radar gauges and waste water treatment plants

### Landuse and topography

The 1992 USGS National Land Cover Data (NLCD) was used as the land cover dataset for this study (EPA, 2004). This dataset was derived from Landsat 5 Thematic Mapper (TM) imagery at the scale of 1:24,000 (30m resolution). The soils exist in these watersheds are more suitable for pasture and rangeland. Hence, the dominant land cover of the study area is rangeland, occupying 42% of the study area. Pasture and Forest

occupy about 18% and 15% of the study area, respectively. Remaining 25% of the study area is occupied by urban and row crops. The rangeland, pasture and forestland undergo various soil and water management practices such as grazing (mainly deferred grazing), root plowing, tree dozing and prescribed burning. The growing cycle of the pasture starts on May 15<sup>th</sup> of a year and ends on November 15<sup>th</sup>, with 2-4 cuttings a year depending on the pattern of rainfall during that year. At the end of the growing cycle, the land is left with at least 0.1m tall of residue at the surface to reduce runoff and erosion. The annual yield of pasture or hay is greater than 2240kg/ha. A visit to the study area by the author suggested that the combination of soil, landuse and landcover, topography make the study area experience hortonian overland flow which is generated by infiltration excess process of the soil.

### **Model description and setup**

Soil and Water Assessment Tool (SWAT) was used to calculate hourly runoff. SWAT employs an infiltration excess method to estimate hourly streamflow. The amount of precipitation that enters the soil by infiltration is calculated using Green & Ampt infiltration (Green & Ampt., 1911) equation which arises from a finite-difference approximation of Darcy's law. The model assumes that there is always ponding of water at the surface thus maintaining a constant pressure head boundary condition. More information about hourly runoff generation using Green & Ampt algorithm can be found at SWAT theoretical manual by Neitsch et al. (2001). Water that does not infiltrate becomes runoff.

Runoff generated on an hourly time step was routed from the upstream area of the watershed to the outlet using the Muskingum routing method. Even though hourly runoff is generated from each Hydrologic Response Unit (HRU, which is defined as a combination of unique soil and landuse), the routing phase is handled by summing the runoff from each HRU to the subbasin outlet. Therefore, the routing phase starts from the subbasin located at the upstream of the watershed and transferred along the length of the channel to the watershed outlet rather than from the upstream HRU. By summing up overland flow generated in each HRU at sub basin level, the effect of soil and Landuse combination in upland flow generation is masked out; thus leads to increase in volume of runoff. In an effort to avoid the possibility of increased runoff volume estimation, Debele (2005) modified SWAT to route hourly runoff on HRU level. The same procedure was adopted in this research to route overland flow from upstream HRU.

### **Weather data collection**

Hourly precipitation data for the years 1999 to 2003 were collected from National Climatic Data Center (NCDC) of National Weather Service for the seven stations in and around the study area having complete precipitation records. Radar data for the study area was obtained from West Gulf River Forecasting Center (WGRFC) for the study period of 1999 to 2003. The hourly data are stage III radar estimates, which were calibrated with surrounding raingauge measurements. Four temperature gauges were located in and around the Upper Trinity River Basin. All other climatic input, such as relative humidity, wind, and solar radiation, were simulated by SWAT weather generator. Streamflow data for the study period of 1999 to 2003 was obtained from

United States Geological Survey (USGS) on an hourly basis. The USGS streamflow gauges, 08043800 and 08043950 were selected with drainage areas of 808 km<sup>2</sup> and 196 km<sup>2</sup>.

### **Data processing**

SWAT can directly use STATSGO data, while SSURGO data has to be preprocessed before input into SWAT. A SWAT-SSURGO extension (Peschel et al., 2003) was used to preprocess SSURGO data to input to SWAT.

From the streamflow data obtained from USGS, the baseflow was separated using a baseflow filter program (Arnold et al., 1995). The base flow recession constant and groundwater delay days, which were calculated from the baseflow filter program, were input to SWAT model to adjust the groundwater flow. Base flow recession constant defines the number of days for base flow to decline through one log cycle and the ground water delay days defines the number of days for the water to reach the shall aquifer from the lowest soil profile (Neitsch et al., (2002)). The calculated values using the base flow filter program showed that on average 19% of streamflow annually is contributed by baseflow, which is about 60 mm of annual average rainfall of 650 mm for the study area.

### ***Optimal radar rainfall extraction method***

In an effort to obtain optimal radar estimates, raw radar data was processed in two different ways. The direct observation of the radar rainfall at the raingauge location was called as the *at-gauge-location* method; while the second method was called the *9-cell minimum difference*. The *9-cell minimum difference method* calculates the radar

rainfall value that shows minimum bias between the gauge and the nine surrounding radar grids.

### ***Calculation of Mean Areal Precipitation (MAP)***

Radar rainfall estimates were averaged over each subbasin to produce MAP using Arc Info-AML language. Calculation of MAP for point rainfall measurements was handled by a different method. The ArcView interface of SWAT assigns rainfall to each subbasin from the raingauge closest to that subbasin. The procedure of selecting rainfall from the closest raingauge facilitates the model to acquire rainfall when very scarce network of raingauges exists for the watershed being studied.

### ***Calculation of conditional and unconditional rainfall with respect to zero***

The precipitation data both from weather radar and raingauges were processed to get conditional and unconditional rainfall. Conditional rainfall, with respect to zero, does not include zero rainfall while unconditional data includes zero rainfall. The reason for splitting the dataset into conditional and unconditional is to analyze the efficiency of radar to capture rainfall that is greater than zero.

### ***Seasonal comparison of radar and raingauge values***

A seasonal comparison of radar and raingauge rainfall allows inferences on the efficiency of radar to capture high rainfall intensities during the summer. This is because the study area receives its highest rainfall during early summer and thus produces the highest volume of runoff over the year. It is also important to assess the ability of radar to capture rainfall reflectivity during both cold and warm seasons of a year. Therefore,

comparison of radar and raingauge values was performed for the spring, summer and fall seasons for the entire five-year period of simulation.

Additionally, radar and raingauge rainfall values were compared on annual basis to evaluate if radar estimates improved due to the improvements in algorithms employed to calculate the rainfall values from the reflectivity. Seasonal and overall precipitation comparison was performed for both conditional and unconditional, with respect to zero, rainfall values.

### ***Bias correction of radar rainfall estimates***

Bias in radar rainfall was calibrated using rainfall from raingauges. An adjustment fact was calculated from optimal radar rainfall which was obtained using *9-cell minimum difference* by following equation:

$$\text{Bias Adjustment Factor (BAF)} = \text{Raingauge Rainfall, mm} / \text{Radar Rainfall, mm} \quad (1)$$

The calculated bias adjustment factor was applied to the raw radar rainfall by three different interpolation techniques; Inverse Distance Weighted (IDW), Spline and Thiessen polygon. Finally the raw radar rainfall was corrected for bias minimization by the following equation:

$$\text{Bias-Adjusted Radar Rainfall, mm} = \text{BAF} \times \text{Raw Radar rainfall (mm)} \quad (2)$$

The hourly raw radar rainfall from 1999 to 2003 was processed using the Arc Info-AML language. The MAP of bias adjusted radar rainfall was obtained by averaging them over each subbasin.



### Comparison statistics

The following statistics were used to compare the rainfall values from radar and raingauge:

#### *Nash-Sutcliff Efficiency (NSE)*

$$NSE = 1.0 - \left( \frac{\sum_{i=1}^N (p_i - o_i)^2}{\sum_{i=1}^N (o_i - \bar{o})^2} \right) \quad (3)$$

Where

$p_i$  = radar estimated rainfall, mm

$o_i$  = raingauge measured rainfall, mm

$\bar{o}$  = Mean of raingauge measured rainfall, mm

NSE varies from negative infinity to 1.0 where values from negative infinity to 0.0 indicate measured rainfall outperforms the radar estimates. Values closer to 1.0 shows closer agreement of radar estimates with raingauge measurements.

#### *Index of Agreement (IOA)*

$$IOA = 1.0 - \left[ \frac{\sum_{i=1}^N (o_i - p_i)^2}{\sum_{i=1}^N (|p_i - \bar{o}| + |o_i - \bar{o}|)^2} \right] \quad (4)$$

The estimated values for the index of agreement of the radar and the raingauge rainfall vary from negative one to 1.0. Values close to negative one shows that the radar rainfall estimates do not agree with raingauge measurements while IOA close to 1.0 suggest radar estimates outperforms raingauge measurements.

Both EE and IOA were calculated for conditional and unconditional rainfall, with respect to zero, for the study period from 1999 to 2003 and also calculated for all three seasons of the year.

### ***Evaluation of SWAT model efficiency in estimating hourly runoff***

#### ***Mean Absolute Error (MAE)***

This function measures the error or bias between observed and simulated runoff in absolute terms. It is defined as,

$$MAE = \frac{1}{n} \sum_{i=1}^n |Q_{o_i} - Q_{s_i}| \quad (5)$$

Where

MAE = Mean Absolute Error, m<sup>3</sup>/sec

n = Number of observations

$Q_{s_i}$  = simulated discharge, m<sup>3</sup> / sec

$Q_{o_i}$  = observed discharge, m<sup>3</sup> / sec

The error between average simulated and average observed runoff shows the amount of deviation of simulated values from the observed values. Smaller error represents the better agreement with observed streamflow.

#### ***Normalized Peak Error (NPE)***

This function calculates the difference between simulated and observed peak discharges and normalizes by observed peak flow, thus giving a relative measure of deviation of simulated peak flow from the observed peak (Masmoudi and Habaieb,

(1993)). A positive NPE shows overestimation of simulated peak flow while negative values show underestimation by predicted runoff.

$$\text{NPE} = \frac{Q_s^{\max} - Q_o^{\max}}{Q_o^{\max}} \quad (6)$$

Where,

NPE = Normalized Peak Error, m<sup>3</sup>/sec

$Q_o^{\max}$  = observed peak, m<sup>3</sup>/sec

$Q_s^{\max}$  = simulated peak, m<sup>3</sup>/sec

Peak runoff plays an important role in designing various hydrologic structures and therefore quantifying the error between observed and SWAT simulated peak runoff becomes significant.

#### *Peak Timing Error (PTE)*

The peak timing error is the difference between observed time-to-peak and simulated time-to-peak. In this study, time to peak was calculated from the peak of rainfall to peak of runoff. It is defined as,

$$\text{PTE} = T_s^{\max} - T_o^{\max} \quad (7)$$

where

PTE = Peak Timing Error, Hours

$T_s^{\max}$  = Simulated time to peak, Hours

$T_o^{\max}$  = Observed time to peak, Hours

Negative PTE shows that simulated peak runoff was produced ahead of observed runoff while positive PTE shows delayed peak generation by simulation. Since, timing of the peak runoff is an important factor in real time flood forecasting, it is needed to analyze the ability of SWAT to produce 0.0 hours of timing error.

*Percentage Relative Volume Error (PRVE)*

$$\text{Percentage Relative volume Error} = \sum_{i=1}^n \frac{Q_{o_i} - Q_{s_i}}{Q_{o_i}} \times 100 \quad (8)$$

Where

$n$  = Number of observations

$Q_{s_i}$  = Simulated runoff,  $\text{m}^3 / \text{sec}$

$Q_{o_i}$  = Observed runoff,  $\text{m}^3 / \text{sec}$

Positive values of PRVE indicate underestimation by simulated runoff while negative percentage values indicate overestimation of simulated runoff volume. Volume of runoff is an important factor in designing hydrologic structures such as reservoirs, weirs and also real time flood forecasting. Therefore, the percentage of volume error needed to be calculated between observed and simulated runoff.

*Nash-Sutcliffe Efficiency (NSE)*

$$\text{NSE} = 1 - \left( \frac{\sum_{i=1}^N (Q_{s_i} - Q_{o_i})^2}{\sum_{i=1}^N (Q_{o_i} - Q_{\text{mean}})^2} \right) \quad (9)$$

Where

$Q_{s_i}$  = Simulated runoff , m<sup>3</sup>/sec

$Q_{o_i}$  = Observed runoff, m<sup>3</sup>/sec

$Q_{mean}$  = Mean of observed runoff, m<sup>3</sup>/sec

NSE measures “the relative magnitude of residual variance to the variance of the flows” (Gupta et al., 1999). NSE ranges from negative infinity to 1.0; values closer to 1.0 being the optimal value. The value of 0.0 indicates that the mean observed streamflow outperforms simulated runoff.

#### *Coefficient of Determination ( $R^2$ )*

A statistic that is widely used to determine the agreement between predicted and observed variable.  $R^2$  represents the fraction of variability in the predicted variable that could be explained by the variation in the observed variable.

$$R^2 = \frac{(\sum Q_{o_i} Q_{s_i})^2}{(\sum Q_{o_i}^2 \sum Q_{s_i}^2)} \quad (10)$$

Where

$Q_{o_i}$  = Observed runoff, m<sup>3</sup>/sec

$Q_{s_i}$  = Simulated runoff, m<sup>3</sup>/sec

$R^2$  varies from 0.0 to 1.0 where values close to 0.0 represents the higher deviation of simulated runoff from the observed.  $R^2$  close to 1.0 show that predicted runoff outperforms observed runoff.

## CHAPTER IV

### RESULTS AND DISCUSSION

The results and discussion section is organized as follows: 1) Selection of optimal radar rainfall extraction methods from one of the following: *at-gauge-location* and *9-cell minimum difference* methods; 2) Seasonal comparison between gauge and optimal radar rainfall estimates; 3) Comparison of conditional and unconditional rainfall, with respect to zero, of raingauge and optimal radar rainfall estimates; 4) Comparison of uncorrected and bias adjusted radar rainfall; 5) Comparison of observed streamflow and SWAT simulated streamflow using various different rainfall inputs: gauge rainfall, uncorrected radar rainfall, bias adjusted radar rainfall using IDW, Spline, and Thiessen polygon methods; 6) Sensitivity analysis.

#### **Selection of optimal radar rainfall estimating method**

Out of seven raingauge stations in and around the study watersheds, two raingauges were selected for rainfall comparison: 1) a gauge named Fortworth, with complete rainfall record and 2) a gauge named Springtown, with missing rainfall records that were replaced by zero or neighboring gauge measurements.

Figures 2 and 3 show the regression plot of raingauge and radar rainfall obtained from *at-gauge-location* and *9-cell minimum difference* methods for stations Fortworth and Springtown, respectively. Although precipitation measurements were compared for the entire study period from 1999 through 2003, to save space, only the results for the year 2003 are presented here.

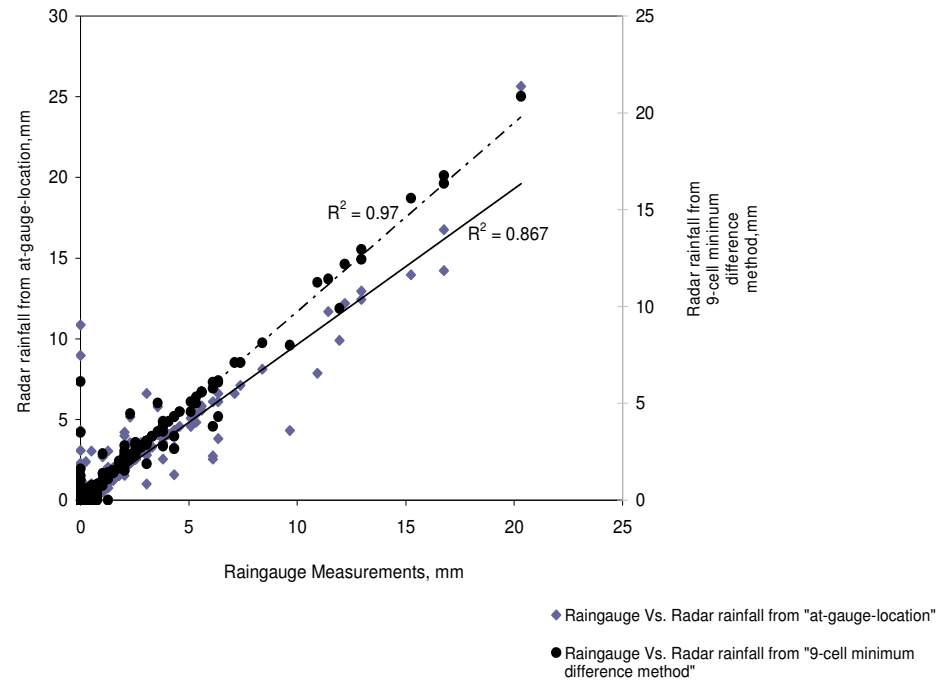


Figure 2. Regression of radar rainfall estimates derived using *at-gauge-location* and *9-cell minimum difference* method for raingauge Fortworth for the year 2003

From Figures 2 and 3 it can be seen that *9-cell minimum difference* method was able to extract optimal radar rainfall estimates better than *at-gauge-location* method. Due to its ability to accommodate the errors raised by deviation of radar location from that of raingauge, and shape and distortion of radar derived rainfall during mapping, *9-cell minimum difference* was able to outperform *at-gauge-location* method. When *at-gauge-location* is used to extract optimal radar rainfall, there is a high possibility that radar may

have detected false rainfall estimates, which is called “Virgo” by National Weather Service (NWS).

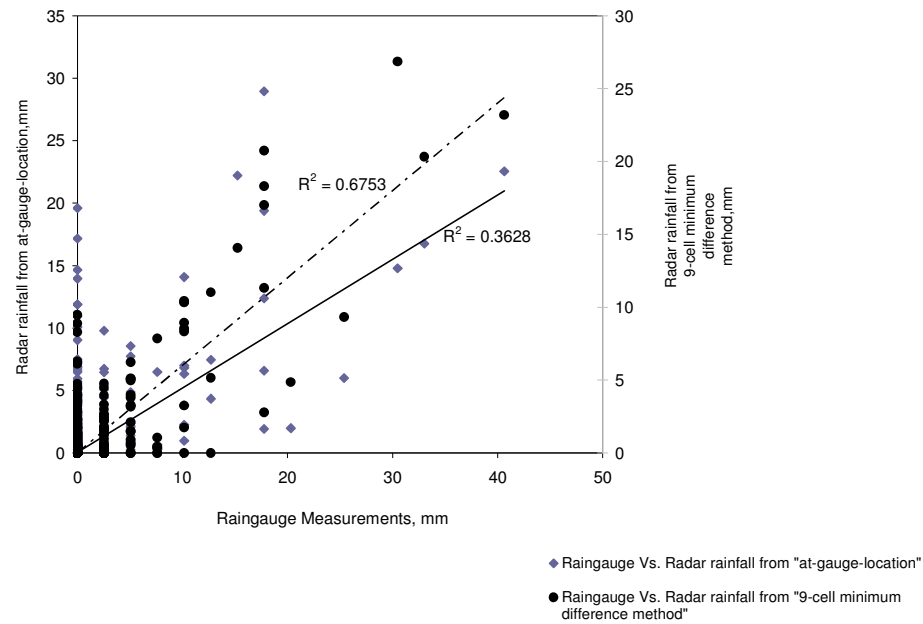


Figure 3. Regression of radar rainfall estimates derived using *at-gauge-location* and *9-cell minimum difference* method for raingauge Springtown for the year 2003

Because weather radars do not actually capture rainfall that falls on the ground, rather it detects reflectivities from mid-air thus; it could have detected rainfall that never reached the ground. To avoid selecting these “Virgo” as rainfall, the 3x3 analysis window applied in the *9-cell minimum difference* method helped to minimize these errors by selecting the radar rainfall estimates that shows minimum bias with raingauge. Hence,



from hereon, the optimal radar rainfall from *9-cell minimum difference*, termed as optimal radar rainfall estimates, was used for further precipitation analysis.

### **Seasonal comparison of raingauge and optimal radar rainfall measurements**

Raingauge and optimal radar rainfall measurements were analyzed individually each season: spring, summer, and fall over the entire period from 1999 to 2003 to characterize the ability of these two sources to capture rainfall across different periods of the year. Because Young et al., (1999) proved that radar rainfall underestimated rainfall during the cold season more than in the warm season. Besides, the study catchments receive their high intensity rainfall events during late spring through early fall. Therefore, seasonal comparison can facilitate the characterization of the ability of gauge and radar to capture these high intensity rainfall values. Albeit both Index of Agreement (IOA) and Coefficient of Efficiency (COE) statistics were calculated over the study period, only COE is presented in this paper. Figure 4 is the plot of distribution of COE for each station for three seasons of 2003. It shows that raingauge measurements and optimal radar rainfall estimates during summer presents higher COE, which ranges from 0.28 to 0.99, than that of spring and fall seasons.

The reason is that the weather radars tend to capture more high intensity rainfall events and its variability across their umbrella than the raingauges (Young et al., (1999)). The COE distribution of the spring season explains the ineffectiveness of gauges to capture low intensity rainfall events whereas radar could have captured those low rainfall values. While four out of seven stations showed good agreement between gauge and optimal radar rainfall for this season, for stations such as Reno, Springtown,

and Lake Bridgeport, the COE varied from -2.29 to 0.01. The reason for these low agreement indices can be attributed to the distance of the raingauge from center of radar. Reflectivities detected at far ranges of radar may tend to estimate low rainfall values, since the accuracy of radar decreases at far ranges. COE distribution for the fall season shows good agreement between raingauge and optimal radar rainfall measurements except for the raingauge Jacksboro.

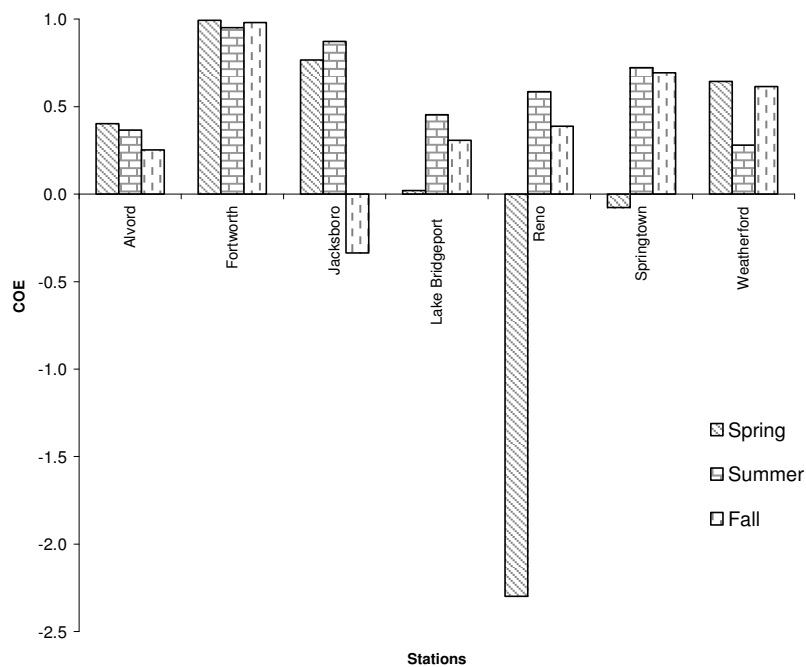


Figure 4. Seasonal comparison of raingauge and optimal radar rainfall estimates for the year 2003

### Conditional analysis of rainfall with respect to zero

The purpose for analyzing conditional and unconditional rainfall, with respect to zero, from gauge and weather radars is to compare the ability of radar and gauge to capture rainfall events that are greater than zero. In addition, runoff producing rainfall events fall in the category of greater than 0.0 mm, which is 25.4 mm for the study watersheds. Gauge and optimal radar rainfall values at raingauges Fortworth and Springtown for the year 2003 were selected to present in this paper. Figures 5 and 6 show the regression of raingauge and optimal radar rainfall measurements for selected raingauge locations.

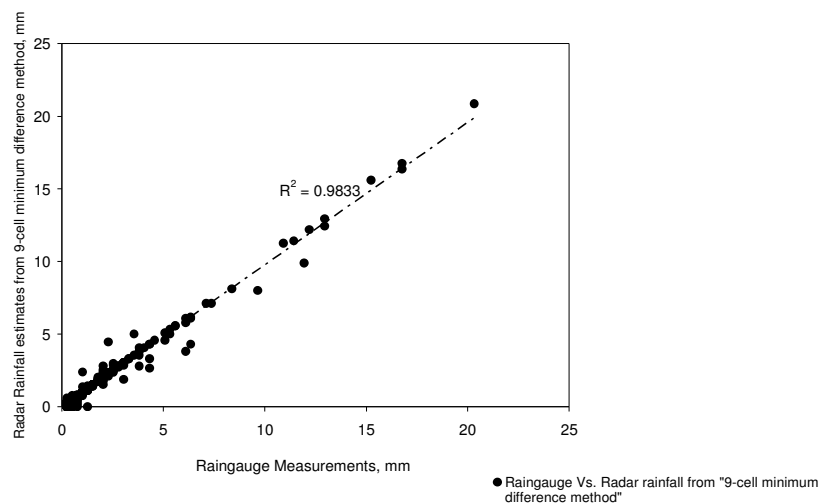


Figure 5. Regression of conditional optimal radar rainfall estimates with rainfall measurements, with respect to zero, of raingauge Fortworth for the year 2003

Compared against Figures 2 and 3, where the regression was calculated using unconditional rainfall, higher coefficient of determination of 0.98 and 0.69, and low dispersion of rainfall traces along the straight line, in Figures 5 and 6 show that both raingauge and radar were able to capture rainfall events greater than 0.0mm. Figure 7 shows the seasonal comparison of conditional raingauge and optimal radar rainfall measurements, with respect to zero, for the year 2003. Six out of seven raingauges depicts the negative COE distribution during spring as result of inability of gauge to capture low intensity of rainfall occurs during that season when radar might have detected these low intensity rainfall.

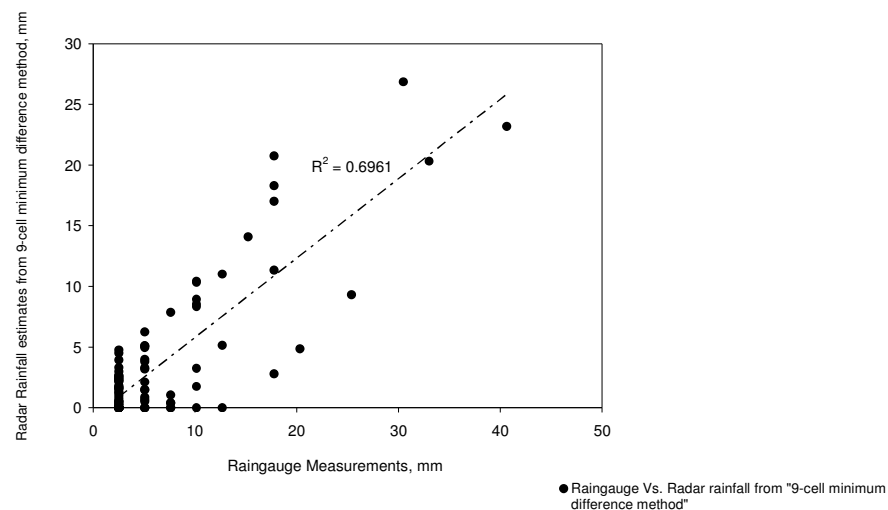


Figure 6. Regression of conditional optimal radar rainfall estimates with rainfall measurements, with respect to zero, from raingauge Springtown for the year 2003

As a point measurement technique, raingauges fail to represent the spatial variation of rainfall across space; while weather radars improved rainfall estimation procedure, even the small spatial variation in rainfall across the space and time can be captured adequately.

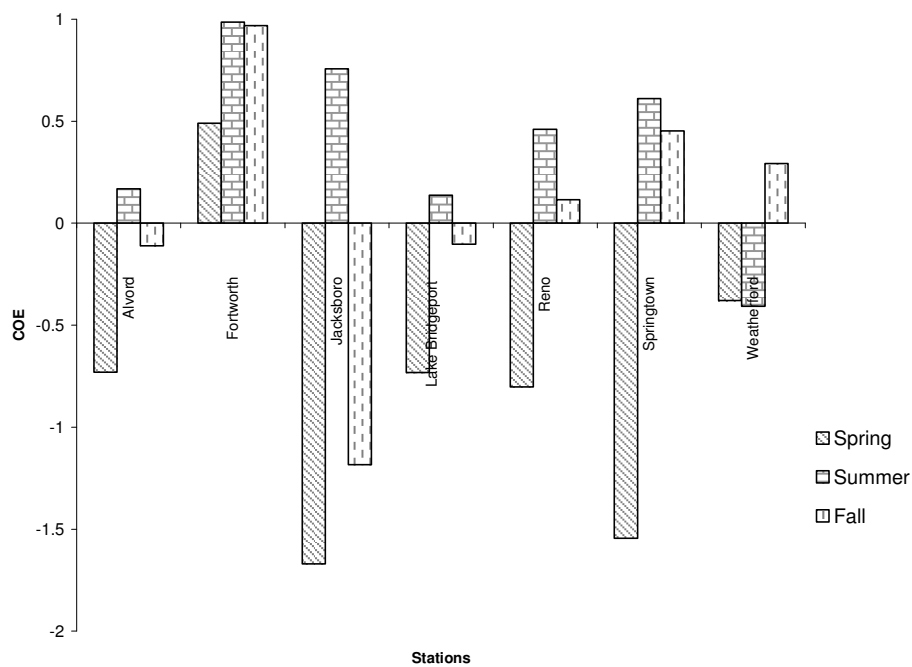


Figure 7. Seasonal comparison of conditional raingauge and optimal radar rainfall estimates, with respect to zero, for the year 2002

As explained in the seasonal comparison of rainfall, high intensity rainfall occurs during summer in the study watersheds. The conditional rainfall analysis, with respect to zero, observed from Figure7 shows promising COE distribution for six out of seven

stations. For raingauge Weatherford, the negative COE distribution which was observed during summer, suggests that quality of radar and gauge rainfall data has to be revised before adopting them for rainfall comparison and applications pertinent to hydrologic modeling. Four out of seven raingauges show negative COE distribution for the fall season. It shows the ability of radar and the inability of gauge to record low intensity of rainfall that occurs during the fall season.

### **Comparison of uncorrected and bias adjusted optimal radar rainfall measurements**

Optimal radar rainfall estimates were corrected for biases and arise from systematic difference in radar and at far ranges from radar. Bias adjusted optimal radar estimates were compared against raingauge observation on a monthly scale. While hourly rainfall for the years 1999 to 2003 was corrected for bias using IDW, Spline, and Thiessen polygon methods, only comparison statistics for the year 2002 is presented in Tables 1 and 2 for both Big Sandy Creek and Walnut Creek Watersheds, respectively.

Normalized peak error defines the relative difference in the maximum rainfall obtained from weather radar to the measured rainfall while estimation bias presents the relative difference between gauge and radar rainfall obtained for each month. Estimation bias observed from Table 1 shows that the differences in rainfall estimates from five different rainfall sources vary greatly across each month of a year. Since rainfall values greater than 25.4 mm is capable of generating runoff in the study catchments, the period from early spring through early fall that received high intensity rainfall values were explained in detail in this section. Estimation bias from April to October (Table 1) shows that uncorrected optimal radar rainfall underestimates rainfall to a lesser amount

compared to bias adjusted rainfall sources. Bias adjusted optimal radar rainfall using IDW depicts overestimation of rainfall during July through October and optimal radar rainfall derived from Spline shows overestimation from September through October. Underestimation of rainfall occurred during the period April to June from optimal radar rainfall obtained using Spline and Thiessen polygon methods.

Differences in peak rainfall amounts from all five different rainfall sources (Table 1) show that uncorrected radar overestimated rainfall over the year. Bias adjusted optimal radar rainfall using Thiessen polygon shows minimum peak error while radar estimates that Spline and IDW methods provided optimal peak rainfall in combination of over- and underestimation. Especially during the high intensity rainfall events, bias adjusted optimal radar rainfall derived using IDW overestimated to a greater extent than that of the Spline method. In general, optimal radar rainfall estimates derived using Thiessen polygon method shows minimum bias against raingauge measurements.

Table 2 shows the estimation bias and normalized peak error of five different rainfall sources for Walnut Creek Watershed. Estimation bias in radar rainfall over months show that bias adjusted radar rainfall estimates obtained using Thiessen polygon method provided minimum error against rainfall derived from IDW and Spline methods. Normalized peak errors for bias adjusted optimal radar rainfall were minimum compared to uncorrected radar rainfall.

Since, one of the objectives of this study was to evaluate the effectiveness of spatially distributed, bias minimized rainfall in generating hourly runoff, the

observations made in the above section will be explained based on the effect of those differences in simulated runoff.

### **Comparison of simulated runoff using five different rainfall inputs**

In this section, rainfall-runoff event analysis will be presented for the study watersheds. Although simulation was done for a five year period, two years of ‘warm-up’ period was allowed to set up models’ initial boundary conditions for runoff generation. Therefore, only three years of the generated runoff was used in output analysis. Efficiency of SWAT was analyzed in a continuous manner rather than single events, which means that model was calibrated over the entire simulation period of 1999 to 2003. Threshold rainfall values greater than 12.7 mm were used in selecting the rainfall-runoff event analysis.

Tables 3a, 3b, and 4a, 4b present the rainfall events that were observed to produce runoff for both Big Sandy Creek and Walnut Creek Watersheds. The tables also present the maximum rainfall observed during that event, the time of occurrence of the peak rainfall, and the distribution of rainfall over the event period for raingauge, uncorrected optimal radar, and bias adjusted optimal radar rainfall measurements. From Tables 3a through 4b, it was observed that the amount of uncorrected optimal radar rainfall during the specified event is always double the amount of bias adjusted optimal radar rainfall values. But, the total amount of bias adjusted optimal radar rainfall derived using Thiessen polygon method for Big Sandy Creek Watershed was much less than even gauge measured rainfall. It is due to the sparse raingauge density (seven raingauges) used for creating Thiessen polygon that were created across the study



Table 1. Monthly rainfall analysis between gauge and uncorrected, bias adjusted optimal radar estimates for the year 2002 for Big Sandy Creek Watershed

| Months           | Normalized Peak Error, mm        |                              |                                 |                                | Estimation Bias, mm              |                              |                                 |                                |
|------------------|----------------------------------|------------------------------|---------------------------------|--------------------------------|----------------------------------|------------------------------|---------------------------------|--------------------------------|
|                  | Gauge Vs<br>Radar<br>Uncorrected | Gauge<br>Vs<br>Radar-<br>IDW | Gauge<br>Vs<br>Radar-<br>Spline | Gauge Vs<br>Radar-<br>Thiessen | Gauge Vs<br>Radar<br>Uncorrected | Gauge<br>Vs<br>Radar-<br>IDW | Gauge<br>Vs<br>Radar-<br>Spline | Gauge Vs<br>Radar-<br>Thiessen |
| <b>January</b>   | 3.26                             | 1.05                         | 1.16                            | 4.49                           | 1.66                             | 4.38                         | 1.60                            | 1.53                           |
| <b>February</b>  | 1.30                             | -0.32                        | -0.31                           | 0.48                           | -0.37                            | 0.18                         | -0.58                           | -0.57                          |
| <b>March</b>     | 1.52                             | 0.51                         | 0.70                            | 0.18                           | -0.90                            | -0.70                        | -0.85                           | -0.86                          |
| <b>April</b>     | 2.63                             | 1.23                         | 1.46                            | 0.76                           | -0.99                            | -0.87                        | -0.95                           | -0.94                          |
| <b>May</b>       | 2.13                             | 0.77                         | 0.77                            | 0.71                           | -0.93                            | -0.49                        | -0.82                           | -0.81                          |
| <b>June</b>      | 4.65                             | 1.74                         | 1.65                            | 1.78                           | -0.98                            | -0.88                        | -0.94                           | -0.94                          |
| <b>July</b>      | 5.37                             | 1.48                         | 1.96                            | -0.54                          | -0.85                            | 0.14                         | -0.61                           | -0.59                          |
| <b>August</b>    | 4.14                             | 1.66                         | 1.65                            | 1.36                           | -0.76                            | 0.63                         | -0.55                           | -0.55                          |
| <b>September</b> | 6.42                             | 4.89                         | 3.52                            | -0.99                          | -0.39                            | 8.96                         | 2.67                            | 3.59                           |
| <b>October</b>   | 5.92                             | 2.51                         | 2.47                            | 0.56                           | -0.43                            | 2.96                         | 0.69                            | 0.70                           |
| <b>November</b>  | 3.00                             | 0.85                         | 0.86                            | 8.70                           | -0.78                            | -0.38                        | -0.71                           | -0.69                          |
| <b>December</b>  | 1.88                             | 0.64                         | 1.00                            | 0.47                           | -0.63                            | -0.21                        | -0.61                           | -0.58                          |

Table 2. Monthly rainfall analysis between gauge and uncorrected, bias adjusted optimal radar estimates for the year 2002 for Walnut Creek Watershed

| Months           | Normalized Peak Error, mm        |                              |                                  |                                   | Estimation Bias, mm              |                              |                                  |                                   |
|------------------|----------------------------------|------------------------------|----------------------------------|-----------------------------------|----------------------------------|------------------------------|----------------------------------|-----------------------------------|
|                  | Gauge Vs<br>Radar<br>Uncorrected | Gauge<br>Vs<br>Radar-<br>IDW | Gauge<br>Vs.<br>Radar-<br>Spline | Gauge<br>Vs<br>Radar-<br>Thiessen | Gauge Vs<br>Radar<br>Uncorrected | Gauge<br>Vs<br>Radar-<br>IDW | Gauge<br>Vs.<br>Radar-<br>Spline | Gauge<br>Vs<br>Radar-<br>Thiessen |
| <b>January</b>   | 1.47                             | 1.59                         | 1.62                             | 1.60                              | 1.00                             | 1.19                         | 1.24                             | 1.17                              |
| <b>February</b>  | 0.10                             | 0.17                         | 0.19                             | 0.19                              | -0.32                            | -0.26                        | -0.24                            | -0.25                             |
| <b>March</b>     | 2.37                             | 2.27                         | 2.22                             | 2.30                              | 0.81                             | 0.78                         | 0.76                             | 0.77                              |
| <b>April</b>     | 1.71                             | 1.44                         | 1.73                             | 1.37                              | 0.85                             | 0.74                         | 0.74                             | 0.72                              |
| <b>May</b>       | -0.12                            | -0.15                        | -0.15                            | -0.15                             | 0.51                             | 0.48                         | 0.55                             | 0.54                              |
| <b>June</b>      | 0.97                             | 0.36                         | 0.41                             | 0.25                              | 0.70                             | 0.71                         | 0.72                             | 0.68                              |
| <b>July</b>      | 0.04                             | 0.05                         | 0.06                             | -0.48                             | 0.44                             | 0.52                         | 0.51                             | 0.20                              |
| <b>August</b>    | -0.49                            | -0.56                        | -0.56                            | -0.56                             | -0.43                            | -0.46                        | -0.47                            | -0.47                             |
| <b>September</b> | 0.39                             | 0.37                         | 0.38                             | 0.39                              | 0.56                             | 0.62                         | 0.46                             | 0.60                              |
| <b>October</b>   | 1.10                             | 0.72                         | 0.71                             | 0.81                              | 1.09                             | 1.14                         | 1.13                             | 1.19                              |
| <b>November</b>  | -0.57                            | -0.58                        | -0.60                            | -0.59                             | -0.59                            | -0.58                        | -0.59                            | -0.58                             |
| <b>December</b>  | -0.28                            | -0.24                        | -0.25                            | -0.22                             | -0.13                            | -0.14                        | -0.14                            | -0.14                             |

Table 3a. Maximum rainfall observed from various rainfall sources for selected runoff producing events for Big Sandy Creek Watershed

| Maximum Rainfall, mm and Time the maximum rainfall occurred, Hour |       |      |                       |          |           |          |              |          |                |          |
|---|-------|------|-----------------------|----------|-----------|----------|--------------|----------|----------------|----------|
| Event   | Gauge |      | Radar-<br>Uncorrected |          | Radar-IDW |          | Radar-Spline |          | Radar-Thiessen |          |
|   | Max   | Hr   | Max                   | Hr       | Max       | Hr       | Max          | Hr       | Max            | Hr       |
| 01/18/2001  | 3.8   | 16.0 | 22.4                  | N*(2.0)  | 8.6       | N(1.0)   | 5.2          | N(1.0)   | 6.8            | 23.0     |
| 01/25/2001  | 6.3   | 4.0  | 19.5                  | 3.0      | 12.0      | 1.0      | 12.5         | 1.0      | 0.0            | 0.0      |
| 02/23/2001  | 13.9  | 22.0 | 28.4                  | 19.0     | 14.2      | 18.0     | 12.3         | 18.0     | 1.0            | 4N(4.0)  |
| 04/11/2001  | 8.9   | 1.0  | 31.1                  | 4.0      | 13.8      | 2.0      | 13.2         | 2.0      | 2.5            | N(14.0)  |
| 04/8/2002   | 3.8   | 10.0 | 23.6                  | N(18.0)  | 14.8      | N(17.0)  | 16.1         | N(17.0)  | 0.1            | 3N(8)    |
| 03/20/2002  | 8.9   | 18.0 | 22.0                  | 21.0     | 19.2      | 20.0     | 21.8         | 20.0     | 8.7            | 14.0     |
| 03/30/2002  | 2.5   | 12.0 | 32.0                  | -N(19.0) | 8.1       | -N(18.0) | 8.01         | -N(18.0) | 3.3            | -N(12.0) |
| 04/7/2002   | 3.8   | 10.0 | 23.6                  | 18.0     | 14.8      | 17.0     | 16.1         | 17.0     | 0.0            | 16.0     |
| 04/13/2002  | 7.6   | 11.0 | 27.6                  | 12.0     | 16.9      | 10.0     | 18.6         | 10.0     | 1.9            | 21.0     |
| 05/25/2002  | 0.0   | 0.0  | 32.6                  | 1.0      | 20.2      | -N(22.0) | 20.2         | -N(22.0) | 0.0            | 0.0      |
| 06/4/2002   | 0.0   | 0.0  | 35.9                  | 15.0     | 17.4      | 13.0     | 16.8         | 13.0     | 8.6            | 2N(4.0)  |
| 06/4/2003   | 16.5  | 7.0  | 20.0                  | 9.0      | 10.2      | 5.0      | 11.6         | 6.0      | 10.3           | 5.0      |
| 06/12/2003  | 19.0  | 4.0  | 38.6                  | 2.0      | 15.2      | 1.0      | 15.3         | 1.0      | 15.5           | 1.0      |

\* N - The peak rainfall was observed the next day

-N - The peak rainfall was observed the previous day

Table 3b. Rainfall distribution of the selected runoff producing events for Big Sandy Creek Watershed

| Event      | Total Intensity of Rainfall for events selected for Big Sandy Creek watershed, Hours(Amount of Rainfall, mm) |                                  |                                |                                 |                                |
|------------|--|----------------------------------|--------------------------------|---------------------------------|--------------------------------|
|            | Gauge  | Raw-Radar                        | Radar-IDW                      | Radar-Spline                    | Radar-Thiessen                 |
| 01/18/2001 | 5(12.6)* + 10(25.2)  | 14(33.9)+ 5(37.5)                | 20(29.2)                       | 20(25.0)                        | 5(7.5)                         |
| 01/25/2001 | 3(7.6)+<br>6(13.9)+15(46.9)  | 5(29.6)+ 11(60.1)+ 18(83.5)      | 4(9.2)+11(24.4)+18(47.9)       | 4(9.1)+11(23.7)+18(45.0)        | 0.0                            |
| 02/23/2001 | 4(29.2)  | 6(62.9)+3(22)                    | 6(29.8)+3(0.78)                | 6(27.8)+3(0.79)                 | 0.0                            |
| 04/11/2001 | 6(22.8)  | 6(52.8)                          | 6(25.2)                        | 6(24.7)                         | 5(5.2)                         |
| 02/18/2002 | 2(7.6,0)   | 7(13.8)+3(5.1)+12(50.3)+4(40.8)  | 6(7.5)+3(2.2)+13(34.8)+5(25.8) | 6(7.5)+3(2.6)+13(36.6)+5(27.6)  | 1(0.04)                        |
| 03/20/2002 | 3(6.3)+7(25.3)+4(5.0)  | 24(169.5)+10(4.8)                | 5(15.1)+21(90.3)+6(0.6)        | 5(14.4)+21(83.7)+6(0.4)         | 6(10.2)                        |
| 03/30/2002 | 1(2.5)   | 12(37.4)+7(68)                   | 11(18.7)+10(25.3)              | 11(19.9)+10(21.4)               | 2(0.15)+5(5.4)                 |
| 04/7/2002  | 2(7.6)   | 10(50.1)+4(40.8)                 | 10(27.4)+8(26.4)               | 10(29.3)+8(28.3)                | 1(0.4)                         |
| 04/13/2002 | 2(8.8)   | 5(57.9)                          | 6(20.0)                        | 6(22.2)                         | 6(3.3)                         |
| 05/25/2002 | 0.0  | 5(43.3)                          | 9(31.0)                        | 9(31.0)                         | 0.0                            |
| 06/4/2002  | 0.0  | 1(25.1)+1(12.0)+10(110.6)        | 13(79.3)                       | 13(76.6)                        | 6(0.24)                        |
| 06/4/2003  | 7(50.7)  | 10(80.1)                         | 10(48.0)                       | 10(52.9)                        | 10(49.7)                       |
| 06/12/2003 | 2(8.6)+5(53.2)   | 4(25.1)+5(38.6)+4(4.7)+11(114.8) | 4(7.8)+4(13.3)+3(0.8)+12(41.9) | 4(7.4)+4(13.2)+4(1.03)+12(39.3) | 4(7.1)+4(13.4)+4(0.9)+12(41.3) |

\* - Value outside the parenthesis represents the duration of rainfall in hours and value inside the parenthesis shows the amount of rainfall in mm.

Table 4a. Maximum rainfall observed from various rainfall sources for selected events for Walnut Creek Watershed

| Maximum Rainfall, mm and Time the maximum rainfall occurred, Hour |       |      |           |      |           |      |              |      |                |      |
|---|-------|------|-----------|------|-----------|------|--------------|------|----------------|------|
| Event   | Gauge |      | Raw-Radar |      | Radar-IDW |      | Radar-Spline |      | Radar-Thiessen |      |
|   | Max   | Hr   | Max       | Hr   | Max       | Hr   | Max          | Hr   | Max            | Hr   |
| 03/19/2002  | 8.9   | 18.0 | 30.0      | 19.0 | 29.1      | 18.0 | 28.6         | 18.0 | 29.4           | 18.0 |
| 10/18/2002  | 10.2  | 18.0 | 21.3      | 18.0 | 17.5      | 14.0 | 17.4         | 14.0 | 18.4           | 14.0 |
| 06/13/2003  | 24.2  | 4.0  | 16.9      | 6.0  | 25.4      | 3.0  | 27.5         | 3.0  | 26.7           | 3.0  |
| 09/11/2003  | 26.7  | 11.0 | 16.1      | 11.0 | 23.6      | 11.0 | 25.2         | 11.0 | 24.1           | 11.0 |

Table 4b. Rainfall distribution of the selected runoff producing events for Walnut Creek Watershed

| Event      | Total Intensity of Rainfall for events selected for Big Sandy Creek watershed, Hours(Amount of Rainfall, mm) |                         |                         |                         |                         |
|------------|--|-------------------------|-------------------------|-------------------------|-------------------------|
|            | Gauge  | Raw-Radar               | Radar-IDW               | Radar-Spline            | Radar-Thiessen          |
| 03/19/2002 | 3(6.3)*+7(25.3)+(4(5.0)  | 14(38.2)+6(54.3)+3(6.5) | 14(37.9)+8(54.4)+3(9.2) | 14(37.7)+8(54.1)+3(9.5) | 14(37.5)+8(54.8)+3(9.4) |
| 10/18/2002 | 8(53.3)+2(3.8)   | 11(90.8)+4(23.7)+2(6.4) | 11(93.7)+8(32.3)        | 11(92.8)+8(32.1)        | 11(94.4)+8(32.5)        |
| 06/13/2003 | 6(91.3)  | 10(63.0)+4(3.1)         | 10(79.5)+4(3.2)         | 10(81.5)+4(3.1)         | 10(80.1)+4(3.2)         |
| 09/11/2003 | 9(83.8)+2(6.3)   | 12(57.5)+7(4.5)         | 12(63.3)+8(6.0)         | 12(66.1)+8(6.2)         | 12(64.1)+8(6.1)         |

\* - Value outside the parenthesis represents the duration of rainfall in hours and value inside the parenthesis shows the amount of rainfall in mm.

watershed. The bias adjustment factor was applied to uncorrected radar rainfall that falls within each Thiessen polygon. Because of sparse networks of raingauge density and large watershed areas, the area of Thiessen polygons increased substantially. Hence, the bias adjusted radar rainfall was more uniformly distributed rainfall, thus the spatial

variability was masked out substantially. This subtle spatial variability leads to lower amounts of bias adjusted radar rainfall averaged over each subbasin than raingauge rainfall. Therefore, runoff simulated using bias adjusted optimal radar rainfall from Thiessen polygon method was eliminated from the output analysis. It also explains the reason that Thiessen polygon derived radar rainfall showing minimum errors in the monthly rainfall analysis for Big Sandy Creek Watershed (Table 1).

Since the area of Walnut Creek Watershed is only  $196\text{km}^2$  the effect of the size of Thiessen polygon was smaller than that of for Big Sandy Creek watershed. From Table 4b, it can be seen that the amount and distribution of bias adjusted optimal radar rainfall from Thiessen polygon method was much closer to that derived from IDW and Spline methods. Based on the observations described above, it is distinct that variability of rainfall increases as increasing watershed area even when applying bias minimization techniques. Thus it has to be noted that for radar analysis and hydrologic studies, it is important to select a significant number of raingauges as a ground truth measurement.

Apart from the duration and amount of rainfall, the occurrence of peak rainfall seemed to vary greatly between gauge and radar rainfall measurements. It was noted from Table 3a (Big Sandy Creek Watershed), that raingauge rainfall was observed far ahead of radar rainfall estimates, which can lead to earlier generation of runoff. As the size of the watershed decreases, the phase difference between gauge and radar rainfall estimates decreased substantially (Table 4a). The influence of bias adjustment of

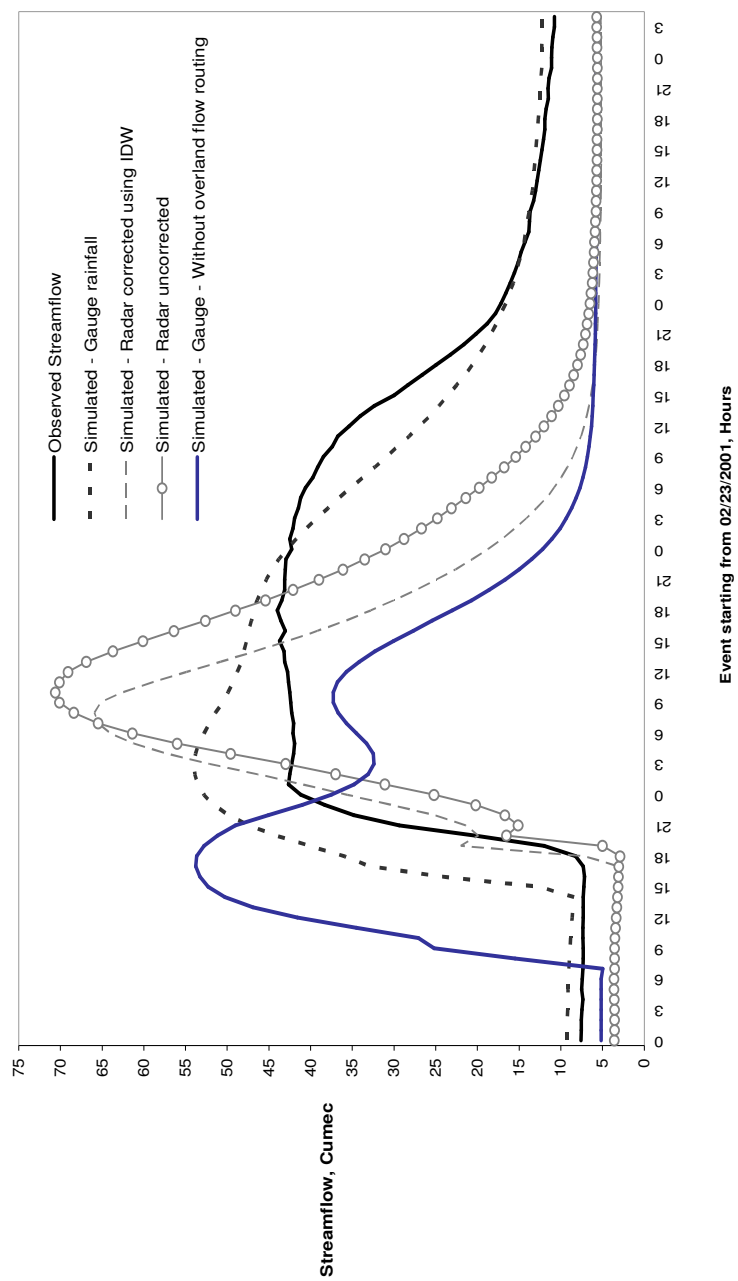


Figure 8. Calibration event selected for Big Sandy Creek Watershed starting on 02/23/2001

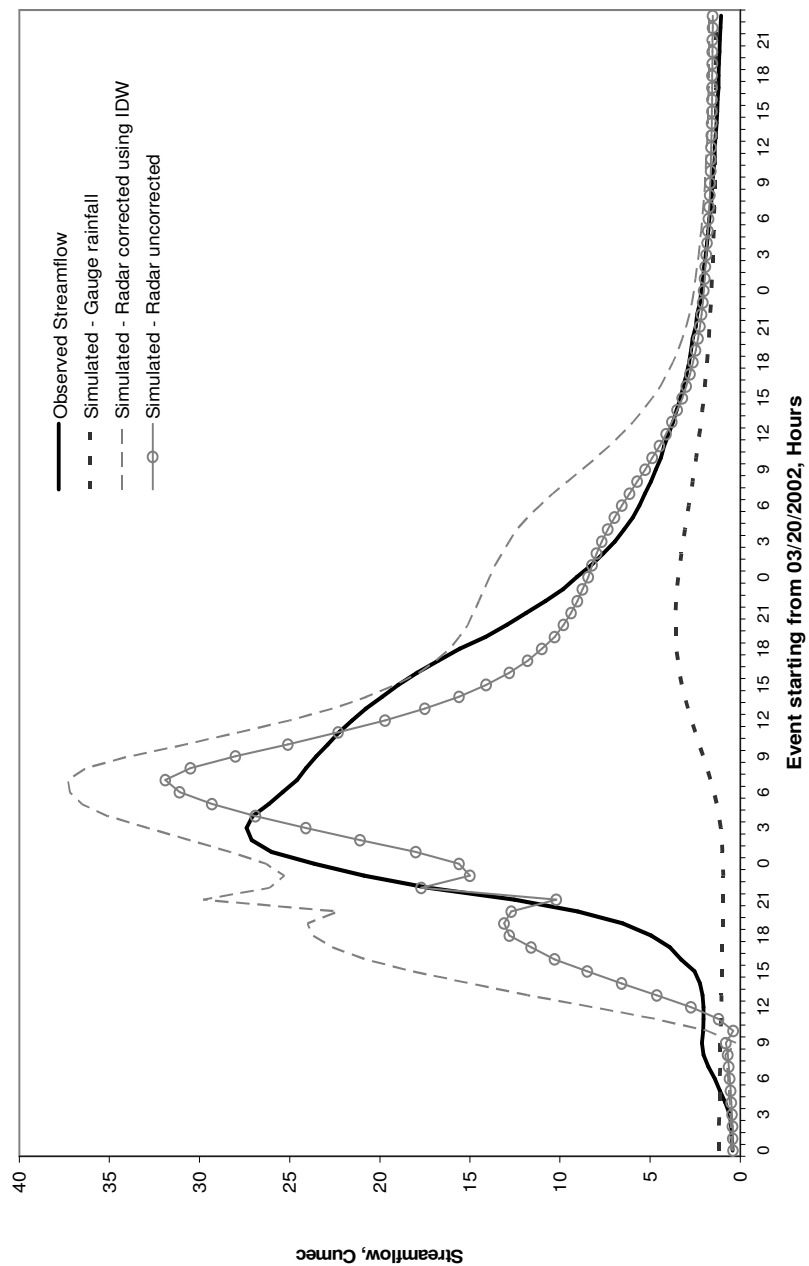


Figure 9. Calibration event selected for Big Sandy Creek Watershed starting on 03/20/2002



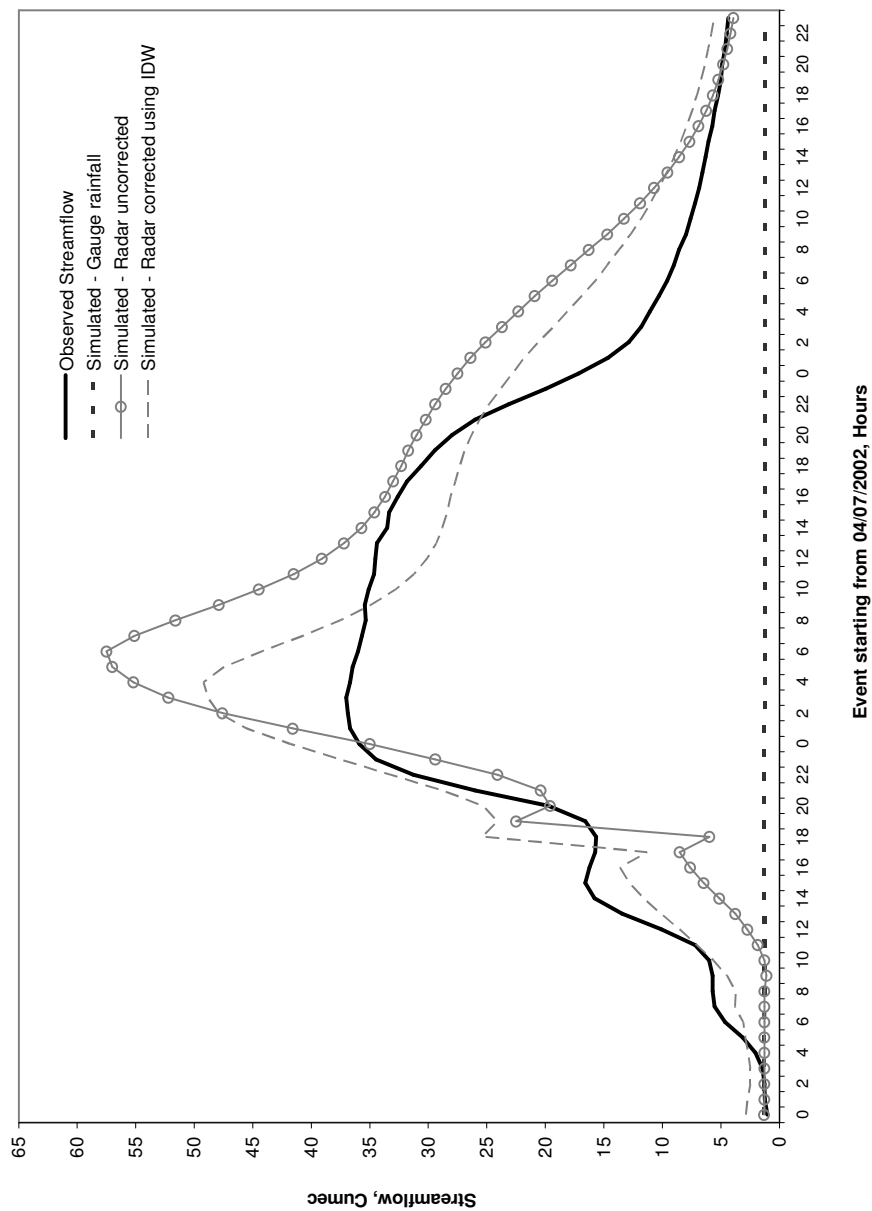


Figure 10. Calibration event selected for Big Sandy Creek Watershed starting on 04/07/2002

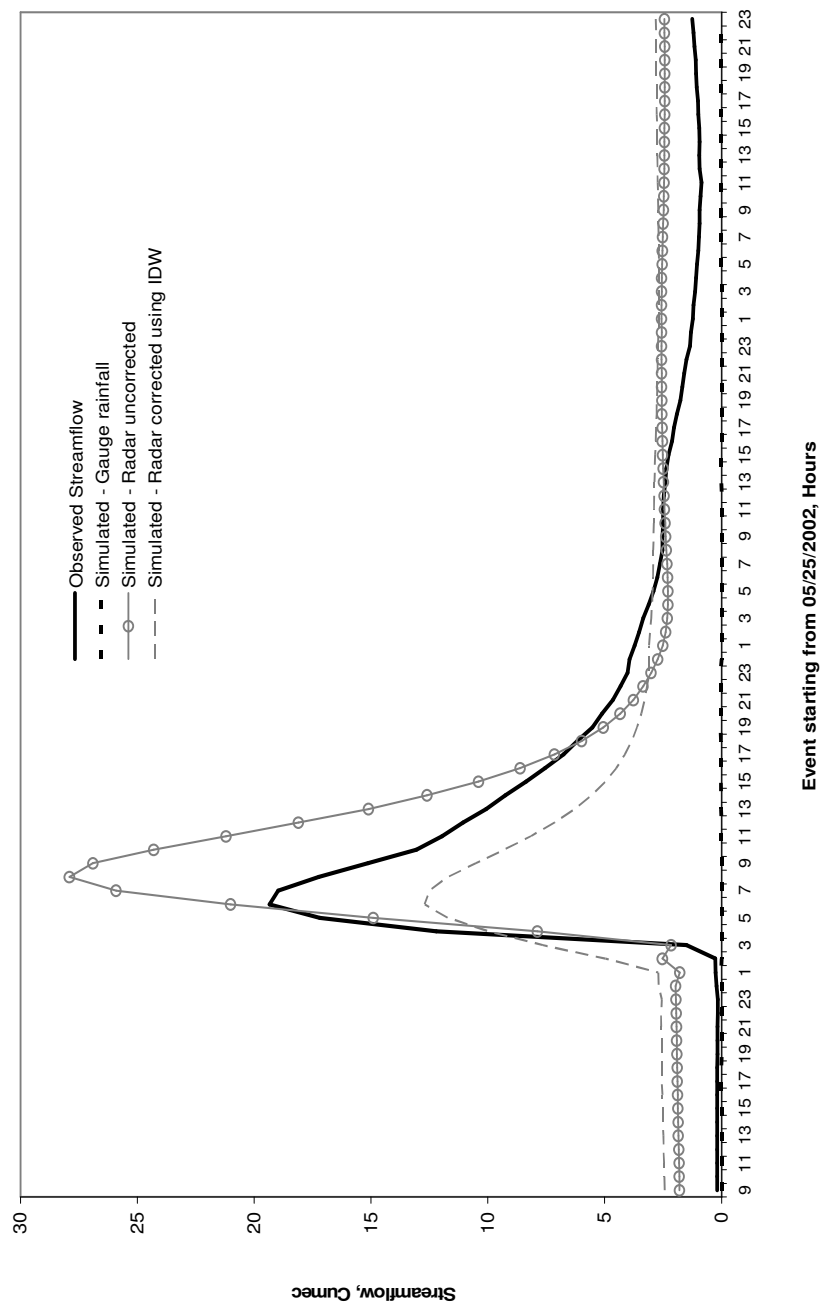


Figure 11. Calibration event selected for Big Sandy Creek Watershed starting on 05/25/2002

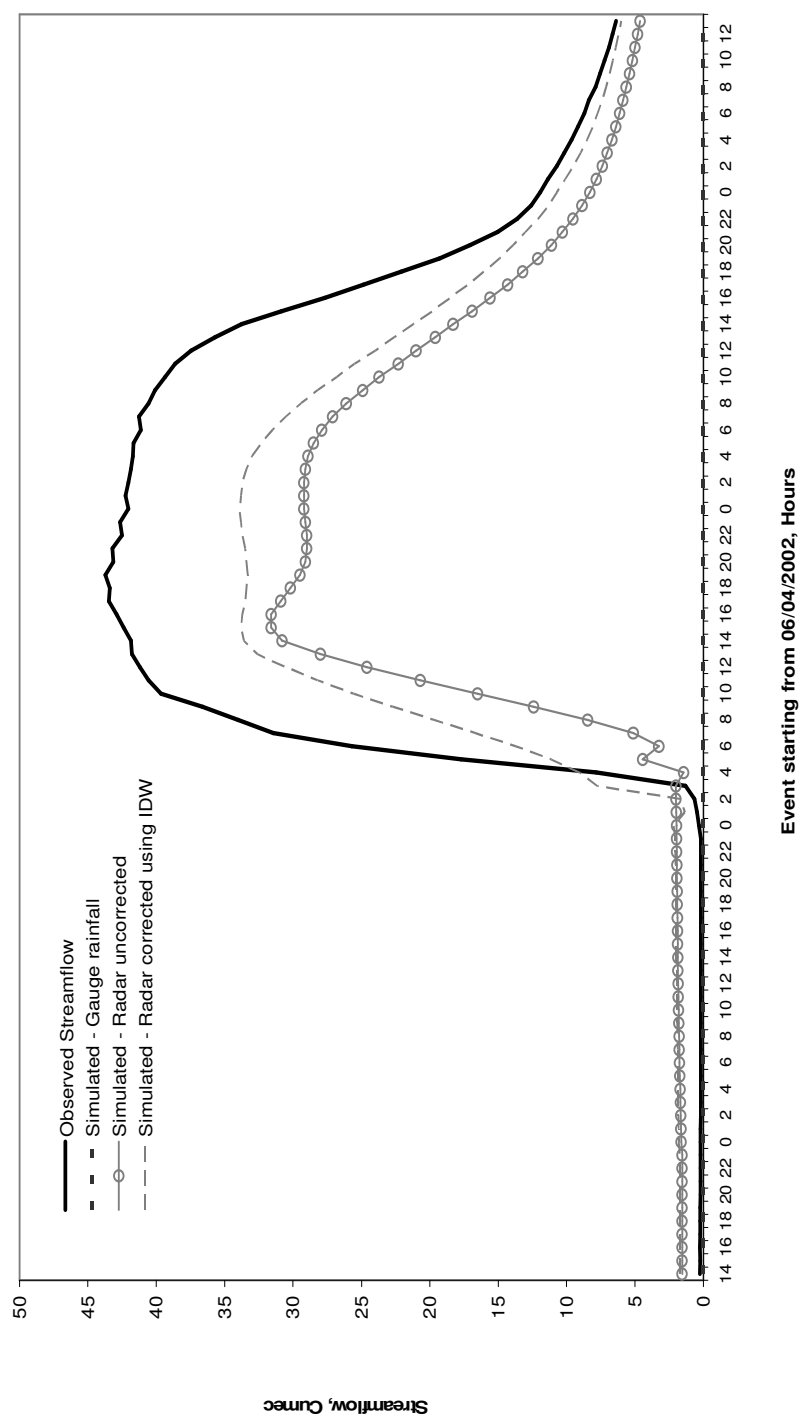


Figure 12. Calibration event selected for Big Sandy Creek Watershed starting on 06/04/2002

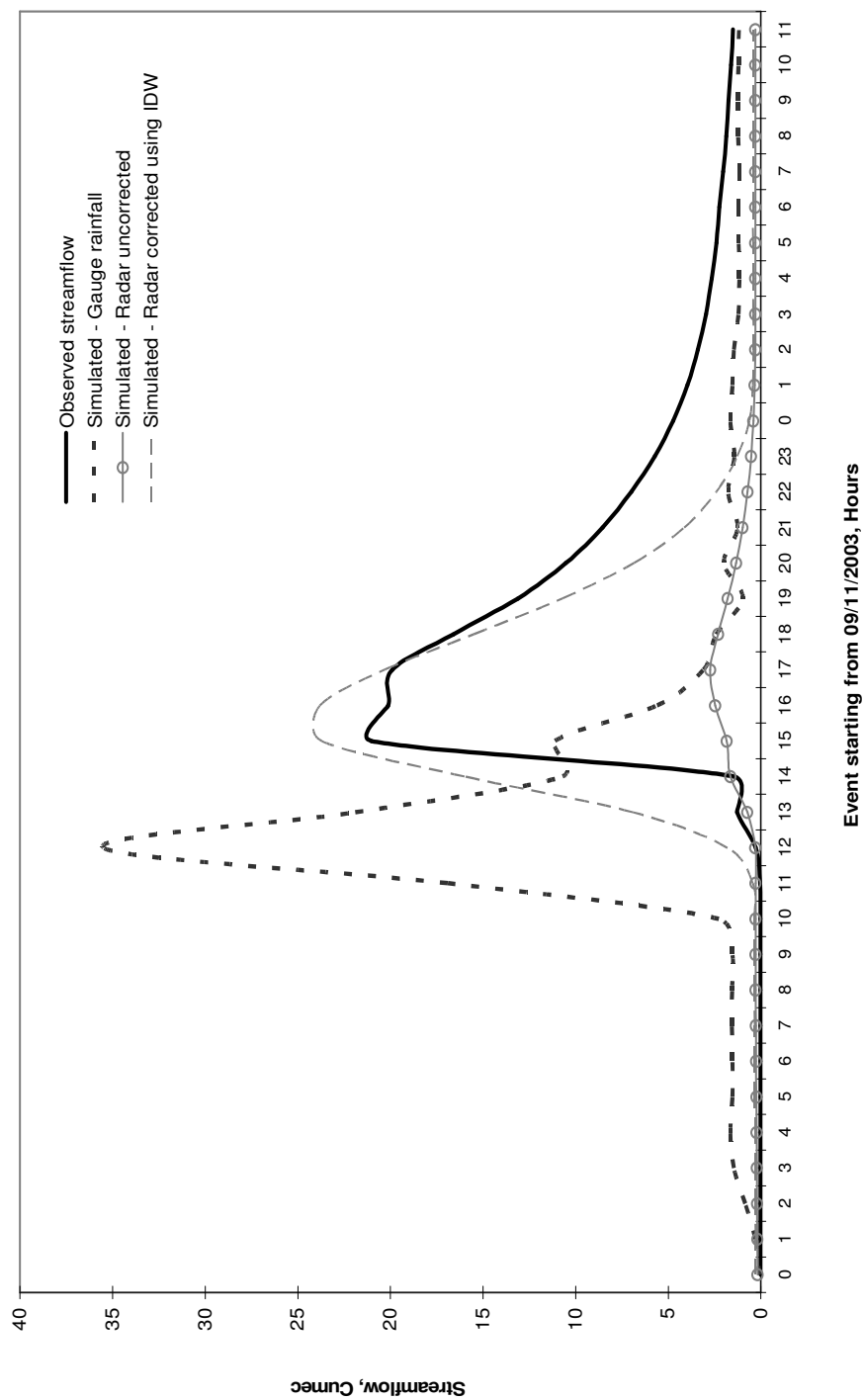


Figure 13. Calibration event selected for Walnut Creek Watershed starting on 09/1/2003

uncorrected optimal radar rainfall was very low as the watershed area decreased as can be seen from Table 4b. Hydrographs from Figures 8 to 12 were generated from Big Sandy Creek Watershed while the hydrograph from Figure 13 was generated for Walnut Creek Watershed. Tables 5 and 6 present the comparison statistics between observed and simulated runoff using various rainfall inputs.

Analyzing statistics between observed and simulated streamflow, Tables 5 and 6 shows that fair agreement exists between observed hydrograph and hydrograph simulated from bias adjusted optimal radar rainfall derived using IDW method. Therefore, in Figures 8 through 13, only hydrographs for observed, uncorrected optimal radar estimates and bias adjusted optimal radar estimates from IDW are presented. In addition, Figure 8 includes the hydrograph generated from gauge rainfall without routing overland flow on an hourly scale (details in Chapter III). When runoff was not routed on a sub-daily basis, volume of the runoff was increased. In addition, runoff started several hours ahead when compared against observed streamflow. The falling limb showed more fluctuations due to the subbasin level water routing.

Figure 8 shows that gauge rainfall was able to reproduce the shape of the observed hydrograph including baseflow; whereas optimal radar rainfall estimates underestimated the baseflow and overestimated peak flow. Normalized peak error (NPE) from Table 5 for this event confirms that error tends to increase for radar rainfall simulated runoff. Also, the Coefficient of Determination,  $R^2$  (RSQ) values tend to decrease for radar rainfall simulated runoff, which in turn proves the poor agreement with observed runoff. The values of RSQ for this event is 0.8 for gauge simulated runoff,

Table 5. Statistics used for comparing observed and simulated streamflow for Big Sandy Creek Watershed

| Source      | Statistics | 1/18/2001 | 1/25/2001 | 2/23/2001 | 4/11/2001 | 2/18/2002 | 3/20/2002 | 3/30/2002 | 4/7/2002 | 4/13/2002 | 5/25/2002 | 6/4/2002 | 4/6/2003 | 6/12/2003 |
|-------------|------------|-----------|-----------|-----------|-----------|-----------|-----------|-----------|----------|-----------|-----------|----------|----------|-----------|
|             |            |           |           |           |           |           |           |           |          |           |           |          |          |           |
| Gauge       | MAE        | 10.7      | 20.6      | 20.5      | 2.9       | 11.3      | 6.0       | 9.5       | 16.4     | 4.3       | 3.4       | 17.4     | 1.6      | 6.4       |
|             | NPE        | 0.9       | 0.8       | 2.2       | 0.5       | 1.0       | 0.9       | 1.0       | 1.0      | 0.9       | 1.0       | 1.0      | 0.1      | 0.7       |
|             | COE        | -0.8      | -0.9      | -191.8    | 0.3       | -0.7      | -0.5      | -0.5      | -1.7     | -1.6      | -0.6      | -1.0     | 0.9      | -0.7      |
|             | PTE        | -2.0      | 9.0       | -15.0     | 2.0       | -4.0      | 15.0      | -2.0      | -2.0     | -1.0      | N/A       | N/A      | 2.0      | 18.0      |
|             | RSQ        | 0.4       | 0.6       | 0.8       | 0.8       | 0.1       | 0.1       | 0.0       | 0.0      | 0.2       | 0.0       | 0.0      | 0.9      | 0.0       |
| Uncorrected | SLOPE      | 0.0       | 0.1       | 1.0       | 0.3       | 0.0       | 0.0       | 0.0       | 0.0      | 0.0       | 0.0       | 0.0      | 1.0      | 0.0       |
|             | MAE        | 8.0       | 18.3      | 22.8      | 3.1       | 4.2       | 1.8       | 6.5       | 6.2      | 15.3      | 1.9       | 7.3      | 4.9      | 17.0      |
|             | NPE        | 0.2       | 0.1       | 2.9       | 0.4       | 0.6       | 0.2       | 0.4       | 0.6      | 6.5       | 0.4       | 0.3      | 0.7      | 3.7       |
|             | COE        | -0.1      | -0.3      | -233.7    | 0.3       | 0.7       | 0.9       | 0.2       | 0.6      | -63.1     | 0.6       | 0.7      | -0.3     | -17.6     |
|             | PTE        | -14.0     | -9.0      | -8.0      | 2.0       | 3.0       | 4.0       | -5.0      | 3.0      | -2.0      | 2.0       | -3.0     | -3.0     | 0.0       |
| IDW         | RSQ        | 0.4       | 0.4       | 0.7       | 0.6       | 0.9       | 0.9       | 0.4       | 0.8      | 0.8       | 0.9       | 0.9      | 0.6      | 0.8       |
|             | SLOPE      | 0.4       | 0.6       | 1.2       | 0.4       | 1.2       | 0.9       | 0.6       | 1.2      | 6.6       | 1.3       | 0.6      | 0.1      | 4.0       |
|             | MAE        | 8.4       | 18.1      | 16.0      | 3.5       | 3.1       | 3.9       | 6.1       | 4.0      | 1.9       | 2.0       | 5.1      | 4.4      | 25.2      |
|             | NPE        | 0.3       | 0.2       | 4.1       | 0.3       | 0.3       | 0.4       | 0.0       | 0.3      | 0.1       | 0.3       | 0.2      | 0.8      | 4.1       |
|             | COE        | -0.2      | -0.3      | -189.6    | 0.1       | 0.9       | 0.5       | 0.3       | 0.8      | 0.6       | 0.7       | 0.9      | 0.1      | -31.1     |
| Spline      | PTE        | -14.0     | -9.0      | -2.0      | 0.0       | 1.0       | 4.0       | -6.0      | 1.0      | -1.0      | 0.0       | -3.0     | 0.0      | -1.0      |
|             | RSQ        | 0.4       | 0.4       | 0.5       | 0.5       | 0.9       | 0.8       | 0.4       | 0.9      | 0.6       | 0.9       | 1.0      | 0.8      | 0.7       |
|             | SLOPE      | 0.3       | 0.7       | 0.9       | 0.4       | 1.0       | 1.2       | 0.5       | 1.0      | 0.5       | 0.5       | 0.7      | 0.2      | 4.6       |
|             | MAE        | 11.3      | 19.4      | 1.0       | 4.2       | 4.8       | 9.6       | 7.1       | 6.8      | 2.7       | 1.8       | 9.8      | 4.2      | 29.2      |
|             | NPE        | 1.0       | 0.5       | 0.9       | 0.4       | 0.3       | 1.2       | 0.1       | 0.3      | 1.1       | 0.1       | 0.5      | 0.8      | 4.6       |
| Spline      | COE        | -1.0      | -0.4      | 0.0       | -0.3      | 0.7       | -2.8      | 0.2       | 0.5      | -0.6      | 0.8       | 0.4      | 0.1      | -40.3     |
|             | PTE        | -16.0     | -9.0      | -12.0     | 0.0       | 1.0       | 2.0       | -6.0      | 1.0      | -1.0      | 0.0       | 5.0      | -5.0     | -1.0      |
|             | RSQ        | 0.8       | 0.4       | 0.4       | 0.5       | 0.9       | 0.7       | 0.4       | 0.9      | 0.6       | 0.9       | 1.0      | 0.7      | 0.7       |
|             | SLOPE      | 0.0       | 0.8       | 0.6       | 0.4       | 1.2       | 2.0       | 0.4       | 1.1      | 1.3       | 0.7       | 0.4      | 0.2      | 5.0       |

Table 6. Statistics used for comparing observed and simulated streamflow for Walnut Creek Watershed

| <b>Rainfall Source</b> | <b>Statistics</b> | <b>03/19/02</b> | <b>10/18/02</b> | <b>06/13/03</b> | <b>09/11/03</b> |
|------------------------|-------------------|-----------------|-----------------|-----------------|-----------------|
| <b>Gauge</b>           | <b>MAE</b>        | 6.61            | 6.75            | 9.87            | 5.68            |
|                        | <b>NPE</b>        | 0.14            | 0.94            | 0.49            | 0.69            |
|                        | <b>COE</b>        | 0.61            | -0.13           | 0.67            | -1.35           |
|                        | <b>PTE</b>        | 0.00            | -2.00           | 0.00            | -3.00           |
|                        | <b>RSQ</b>        | 0.67            | 0.18            | 0.90            | 0.00            |
|                        | <b>SLOPE</b>      | 0.83            | 0.02            | 1.34            | -0.01           |
| <b>Radar</b>           | <b>MAE</b>        | 11.91           | 6.79            | 16.75           | 3.82            |
|                        | <b>NPE</b>        | 0.12            | 0.46            | 0.53            | 0.87            |
|                        | <b>COE</b>        | -0.77           | 0.40            | -0.02           | -0.17           |
|                        | <b>PTE</b>        | 3.00            | 2.00            | 4.00            | 2.00            |
|                        | <b>RSQ</b>        | 0.26            | 0.45            | 0.08            | 0.83            |
|                        | <b>SLOPE</b>      | 0.75            | 0.52            | 0.17            | 0.11            |
| <b>IDW</b>             | <b>MAE</b>        | 9.85            | 5.68            | 20.00           | 2.16            |
|                        | <b>NPE</b>        | 0.17            | 0.38            | 0.10            | 0.13            |
|                        | <b>COE</b>        | -0.29           | 0.55            | -0.18           | 0.70            |
|                        | <b>PTE</b>        | 1.00            | -2.00           | 1.00            | 0.00            |
|                        | <b>RSQ</b>        | 0.53            | 0.59            | 0.62            | 0.76            |
|                        | <b>SLOPE</b>      | 1.14            | 0.65            | 1.13            | 0.98            |
| <b>Spline</b>          | <b>MAE</b>        | 10.27           | 6.69            | 17.49           | 2.15            |
|                        | <b>NPE</b>        | 0.26            | 0.41            | 0.09            | 0.00            |
|                        | <b>COE</b>        | -0.47           | 0.44            | 0.18            | 0.71            |
|                        | <b>PTE</b>        | 2.00            | -2.00           | 1.00            | 1.00            |
|                        | <b>RSQ</b>        | 0.55            | 0.52            | 0.60            | 0.74            |
|                        | <b>SLOPE</b>      | 1.21            | 0.59            | 0.93            | 0.83            |
| <b>Thiessen</b>        | <b>MAE</b>        | 14.17           | 6.99            | 17.69           | 2.16            |
|                        | <b>NPE</b>        | 0.56            | 0.29            | 0.05            | 0.14            |
|                        | <b>COE</b>        | -1.61           | 0.41            | 0.10            | 0.69            |
|                        | <b>PTE</b>        | 2.00            | -2.00           | 0.00            | 0.00            |
|                        | <b>RSQ</b>        | 0.50            | 0.54            | 0.61            | 0.75            |
|                        | <b>SLOPE</b>      | 1.41            | 0.68            | 0.99            | 0.96            |

0.7 and 0.5 for runoff simulated using uncorrected optimal radar rainfall and bias adjusted optimal radar rainfall from IDW. This character of radar rainfall shows that

increase in rainfall leads to increase in volume of runoff; thereby reducing runoff to baseflow ratio for a rainfall-runoff event where water is transported by the system too rapidly to be infiltrated to the soil.

Effect of various rainfall input sources can also be seen from the simulated hydrographs (Figure 9). The amount of gauge rainfall observed for the event occurred on March 20, 2002 was 36.6 mm over nearly 16 hours where 174.8 mm over 35 hours was observed for uncorrected optimal radar rainfall estimates. The maximum observed runoff for this event was approximately  $26 \text{ m}^3/\text{sec}$ . Low intensity of rainfall over long duration from gauges was not able to reproduce the observed hydrograph while uncorrected optimal radar rainfall produced the width and height of the hydrograph similar to the observed one. In contrast to other rainfall-runoff events where bias adjusted optimal radar rainfall reproduces the volume of observed runoff very well, Figure 9 shows that uncorrected optimal radar estimates performs better than bias adjusted optimal radar rainfall. Referring back to the rainfall amount and duration for this event from Table 5, it may be noted that uncorrected optimal radar estimated nearly 174.3 mm of rainfall over 34 hours whereas bias adjusted optimal radar rainfall by IDW detected nearly 32 hours of rainfall with a total of 116 mm. This irregularity in runoff production suggests the importance of distribution and amount of rainfall over a rainfall-runoff event.

Overestimation of runoff by bias adjusted optimal radar rainfall from IDW method is due to the antecedent moisture condition of the soils. The distribution of the rainfall over the first five hours with the total of 15.1mm saturated the soil with enough moisture and thus when 90.3mm of rainfall occurred for next 21 hours continuously, the runoff was



created instantaneously causing a sudden rise of the hydrograph. On the other end, a continuous rainfall amount of 169.5 mm for 24 hours from uncorrected optimal radar rainfall reproduced the observed hydrograph with optimum amount of loss of other hydrological components such as evaporation and transpiration.

Runoff simulated using uncorrected optimal radar rainfall showed high volume difference when compared against observed streamflow volume (Figure 10). But, the optimal radar rainfall, which was corrected for bias showed promising results in terms of volume of runoff. This reduction in volume of runoff is due to the minimization of biases in uncorrected radar rainfall. SWAT also reproduced the real world hydrologic cycle, which may be observed from Figures 11 and 12, 0.0 m<sup>3</sup>/sec of streamflow was simulated when the gauge measured rainfall was 0.0mm.

Figure 11 shows that bias adjusted optimal radar rainfall from IDW underestimated the volume of runoff to a substantial amount due to the reduced amount of rainfall resulted from bias correction. Although, this kind of behavior of bias adjusted rainfall can occur in rare hydrograph events, the statistics from Table 5 show that runoff simulated using bias adjusted optimal radar rainfall from IDW has lower volume, peak errors and higher coefficient of efficiency and coefficient of determination compared to runoff simulated using gauge, uncorrected radar rainfall and bias adjusted radar rainfall from Spline.

Besides the analysis of volume of runoff, phase difference between observed and simulated hydrographs is another factor in determining the efficiency of a hydrologic model. Due to its ability to capture spatial distribution of rainfall across the study area,

runoff produced by both uncorrected and bias adjusted optimal radar rainfall estimates showed improved performance in terms of minimizing the bias in time in generating peak runoff (Figures 8 to 12). Figure 9 clearly shows the phase difference introduced by point measured gauge rainfall where bias adjusted optimal radar rainfall showed no phase difference at all. This statement proves that time of occurrence of maximum rainfall influences the time of peak runoff generation.

When discussing the effectiveness of SWAT to generate baseflow, Figure 11 shows increased volume of baseflow under the hydrograph. Referring back to the distribution and amount of rainfall for Figure 11 from Table 5 reports that average hourly intensity of rainfall is 3.4mm which allows the infiltration of rainfall at a much slower pace to the subsurface thus increasing baseflow. This behavior finally results in reduction of surface runoff.

From Table 5, it may be noted that the average volume runoff errors tend to be reduced as the spatial resolution of rainfall increased. For example, for event starting on April 7, 2002, the average volume error (MAE) in runoff simulated using gauge rainfall is  $16.4 \text{ m}^3/\text{sec}$  whereas runoff generated from uncorrected optimal radar rainfall is  $6.2 \text{ m}^3/\text{sec}$ . The error tends to be reduced to a greater extent when the systematic biases in radar rainfall are reduced. The average runoff error for bias adjusted optimal radar rainfall from IDW and Spline is  $4 \text{ m}^3/\text{sec}$  and  $6.8 \text{ m}^3/\text{sec}$ , respectively. The error in peak runoff is also reduced as the biases in radar rainfall are minimized, which may be noted from NPE for the event occurred on June 4, 2002. The NPE for gauge rainfall simulated runoff is  $1.0 \text{ m}^3/\text{sec}$  while that of runoff simulated using uncorrected optimal radar

rainfall is  $0.3 \text{ m}^3/\text{sec}$ . Minimum NPE ( $0.2 \text{ m}^3/\text{sec}$ ) is observed for simulated runoff using radar rainfall from IDW method.

Runoff simulated from spatially distributed rainfall showed fair agreement with observed runoff than the point measured gauge rainfall. Table 5 shows that for a rainfall-runoff event that occurred on February 18, 2002, runoff simulated from gauge rainfall has COE of -0.7 whereas runoff simulated using optimal radar rainfall estimates, both uncorrected and bias adjusted, have COE of 0.7 and 0.9. RSQ for the same event is 0.1 for gauge rainfall simulated runoff, 0.9 for both uncorrected bias adjusted optimal radar rainfall simulated runoff estimates. An event occurred during June 12, 2003 that showed good agreement with observed runoff with a RSQ of 0.8, 0.7 for runoff simulated using uncorrected and bias adjusted optimal radar estimates from IDW, respectively. Whereas the RSQ of runoff simulated from gauge rainfall is 0.0 which describes the poor representation of gauge rainfall for this event.

Analysis of event statistics for Walnut Creek Watershed (Table 6) presents that average runoff volume error increases as the amount of rainfall increases. For example, an event that occurred on June 13, 2003 had a MAE of  $9.87 \text{ m}^3/\text{sec}$  for runoff simulated using gauge rainfall whereas the error tend to increase for spatially distributed radar rainfall. Uncorrected optimal radar rainfall estimates simulated runoff has an error of  $16.75 \text{ m}^3/\text{sec}$ , while runoff simulated from bias adjusted optimal radar rainfall estimates using IDW, Spline, and Thiessen polygon methods has an error of  $20 \text{ m}^3/\text{sec}$ ,  $17.49 \text{ m}^3/\text{sec}$  and  $17.69 \text{ m}^3/\text{sec}$ , respectively. For the same event, the simulated peak runoff

error tends to decrease as the spatial variability of rainfall increases. COE and RSQ values also decrease as increase in spatial resolution of rainfall.

Aforementioned observations show that as the area of watershed increases, the spatial variability of rainfall becomes a significant factor in runoff generation. Albeit the number of raingauges used for both watersheds are equal (which is two), effects of rainfall from these gauges affected the generation of runoff in different modes. The only factor that may be attributed to this behavior is the size of the watersheds, which purely confirms the conclusions by Koren et al. (1999). Therefore, density of raingauge networks is “the” most important factor in generation of runoff. The degree to which the density of raingauge network is considered as the significant factor is more pronounced as the area of the catchment increases.

Besides the effect of spatial variability of rainfall, runoff producing model structure also plays a vital role in runoff process. It has been proved by the researchers that infiltration excess models are more sensitive to errors in radar rainfall estimates (Winchell et al., 1998); which can be better explained by Figure 12. From this figure, it may be noted that 69.3 mm of bias adjusted IDW derived optimal radar rainfall with the duration of 20 hours shows fair agreement with observed hydrograph whereas 62 mm, 19 hours of uncorrected optimal radar rainfall was not able to reproduce the observed runoff.

From the rainfall-runoff events selected for this study it is noted that SWAT produced more flashy start and/or fluctuations in the rising limb of the simulated hydrographs. This behavior also may be due to the Green & Ampt infiltration algorithm,

which models infiltration. From a study by Serrano, E. (2004), it was concluded that Green & Ampt model produces earlier time to ponding and thus more rapid decline in infiltration rate due to assumption of constant pressure head at the wetting front. Decreasing infiltration rate increases amount of runoff thus giving a flashy start in the rising limb of the SWAT simulated hydrographs. He also notes that Green & Ampt model creates a sustained higher infiltration rate after a prolonged wet period during a rainfall-runoff event, which will be a noteworthy feature of a falling limb of a hydrograph. Aforementioned characters of the Green & Ampt model can be clearly seen in Figure 13. Increasing infiltration rate for a longer period reduces runoff volume; and thus creating a sudden reduction of runoff in the falling limb of the hydrograph. The same behavior can be observed from Figures 8 to 12.

### **Sensitivity analysis**

Sensitivity of the model to various hydrological parameters was analyzed by using SWAT models' "Sensitivity Analysis" tool. Table 7 presents the results of the sensitivity analysis. Although both Big Sandy Creek and Walnut Creek Watersheds were used for this analysis separately, a summary of the parameters and parameter ranges are given in Table 7. Calibration was done based on the values suggested in the table to reproduce the actual hydrologic cycle rather than just curve fitting of the hydrographs. Based on the observations from the sensitivity analysis, the model was more sensitive to the ESCO, the soil evaporation factor. Since the primary landuse in the study catchments is rangelands, it was noted from the sensitivity analysis that evaporation-transpiration was the key factor in determining the runoff generating process.

Table 7. Parameter range of variables derived from Sensitivity analysis

| Variables | Description  | Range of Values                         |   |
|-----------|--|---|---|
|           |  | Area of Watershed < 200 km <sup>2</sup> | Area of Watershed > 200 km <sup>2</sup> |
| MSK_CO1   | Impact of storage time constant for normal flow  | 0                                       | 0                                       |
| MSK_CO2   | Impact of storage time constant for low flow   | 0.5 - 1.8                               | 1.2 - 1.5                               |
| MSK_X     | Weighting factor that controls the relative importance of inflow and outflow in determining the storage in a reach | 0.2 - 0.3                               | 0.2 - 0.25                              |
| ESCO      | The parameter that will be used to extract more water from lower depths of soil profile to meet evaporative demand | 0.65 - 0.75                             | 0.7 - 0.75                              |
| AWC       | Available Water Content  | Increase or Decrease by 20%             | Increase or Decrease by 15%             |
| SOL_K     | Saturated hydraulic conductivity   | Increase or Decrease by 25 - 45%        | Increase or Decrease by 25%             |
| GW_REVAP  | Evaporation of water to overlying unsaturated zone from the saturated zones below                                  | 0.02 - 0.18                             | 0.1 - 0.2                               |
| ALPHA_BF  | Baseflow alpha factor  | 0.3 - 0.4                               | 0.008 - 0.013                           |
| CN2       | Initial SCS runoff curve number for moisture condition II  | Increase or Decrease by 15%             | Increase or Decrease by 10%             |

## CHAPTER V

### CONCLUSION

Spatial variability of rainfall is the major source of uncertainty in hydrologic and water quality modeling outputs. Therefore, this research focused on evaluating the effectiveness of Soil and Water Assessment Tool (SWAT) in sub-daily runoff estimation using point rainfall measurements and spatially distributed weather radar rainfall estimates for two watersheds in North Central Texas. In an effort to analyze the effect of rainfall spatial variability, a watershed with an area of 808 km<sup>2</sup>, named Big Sandy Creek and another watershed with an area of 196 km<sup>2</sup>, named Walnut Creek Watershed were selected for this study. Regardless of improved spatial resolution of radar rainfall, various biases exist in the estimates due to systematic differences, and rainfall estimation at far ranges of radar location. These biases were minimized by selecting optimal radar rainfall estimates using a novice method called *9-cell minimum difference*. The radar rainfall derived using this method was termed as uncorrected optimal radar rainfall estimates. The bias between raingauge and uncorrected optimal radar rainfall measurements was applied to the radar estimates at a spatial scale of 4 km<sup>2</sup>, using IDW, Spline, and Thiessen polygon methods. Radar rainfall derived from these methods was termed as bias adjusted optimal radar rainfall estimates. Sub-daily runoff was generated using raingauge rainfall, uncorrected optimal radar rainfall, and bias adjusted optimal radar rainfall estimates for the study period of 1999 - 2003.

From the results of this study, the following observations were made regarding uncertainty of rainfall input in runoff generation:

1. Spatial variability of rainfall is a significant factor in determining the accuracy of hydrologic modeling outputs.
2. As the watershed area increases, the intensity of effect of spatial variability is more pronounced in generating runoff. Increasing watershed area masks the spatial variability of rainfall, thus leading to the assumption of uniform rainfall across the watershed.
3. Spatial variability of rainfall from raingauges influences the phase and volume difference in runoff generation. Reduced spatial variability of rainfall from weather radars reduced runoff volume and phase differences.
4. Regardless of the increased spatial resolution, the uncertainty in radar rainfall estimates increased due to biases that arise from the reflectivity values captured from far ranges of radar umbrella, distance between the radar and raingauge location that were used to calibrate the rainfall estimates, and detection of reflectivity close to mid-air rather than measuring it near the ground. Therefore, an optimal radar rainfall extraction method has to be employed when radar rainfall is used in hydrologic modeling in order to increase the accuracy of hydrograph generation.
5. Increase in bias in radar rainfall estimates increased the volume of runoff, whereas bias adjusted radar rainfall showed promising results in terms of volume of hydrograph. Therefore, an optimal bias minimization procedure should be adopted to derive accurate radar rainfall.



6. In addition to the input uncertainty, runoff producing algorithm and routing methods are key factors in increasing the uncertainty in model outputs. If the rainfall excess is estimated accurately and routed along the main channel to the catchment outlet, the hydrologic parameters can distinctly reproduce the real world hydrologic cycle.
7. Results from this study also suggested that runoff estimation on a fine temporal scale has to be modeled carefully. Since volume of runoff is the key factor in deciding a hydrological model's efficiency, various hydrologic components such as overland flow, evapotranspiration, and groundwater flow in SWAT has to be derived on an hourly scale rather than on daily basis. At present, SWAT generates and routes overland flow and evapotranspiration on a daily scale rather than an hourly basis, which leads to overestimation of volume of runoff. Modifications have to be made to these components in order to estimate runoff accurately. In addition, groundwater flow is assumed to be distributed uniformly over a day in SWAT, which in turn increases the uncertainty in volume of runoff where watershed processes are dominated by baseflow. Therefore, generation and routing of groundwater flow has to be handled on a fine temporal scale when runoff is simulated on a fine spatial and temporal scale.

## REFERENCES

- Arnold JG, Allen PM, Bernhart G. 1993. A comprehensive surface-groundwater flow Model. *Journal of Hydrology* **142**(1-4): 47-69.
- Arnold JG, Allen PM, Muttiah R, Bernhardt G. 1995. Automated baseflow separation and recession analysis techniques. *Ground Water* **33**(6): 1010-1018.
- Arnold JG, Potter KN, King KW, Allen PM. 2005. Estimation of soil cracking and the effect on surface runoff in a Texas Blackland Prairie watershed. *Hydrological Processes* **19**: 589-603.
- Bacchi B, Kottegoda NT. 1995. Identification and calibration of spatial correlation patterns of rainfall. *Journal of Hydrology* **165**: 311-348.
- Bedient PB, Holder A, Benavides JA, Vieux BE. 2004. Radar-based flood warning system applied to tropical storm allison. *Journal of Hydrologic Engineering* **8**(6): 308-318.
- Benaman J, Shoemaker CA. 2005. An analysis of high-flow sediment event data for evaluating model performance. *Hydrological Processes* **19**: 605-620.
- Borga M. 2002. Accuracy of radar rainfall estimates for streamflow simulation. *Journal of Hydrology* **267**: 26-39.
- Chaubey I, Haan CT, Salisbury JM, Grunwald S. 1999. Quantifying model output uncertainty due to spatial variability of rainfall. *Journal of American Water Resources Association* **35**(5): 1113-1123.
- Chow VT, Maidment DR, and Mays LW. 1988. *Applied Hydrology*. McGraw-Hill Science/Engineering/Math; New York: 71.
- Creutin JD, Delrieu G, Lebel T. 1988. Rain measurement by raingage-radar combination: a geostatistical approach. *Journal of Atmospheric and Oceanic Technology* **5**: 102-115.
- Debele BN. 2005. Better insight into water resources management through integrated upland watershed and downstream waterbody hydrodynamic and water quality models (SWAT & CE-QUAL-W2). PhD Dissertation submitted to Cornell University, Ithaca, NY.
- Durrans SR, Julian LT, Yekta M. 2002. Estimation of depth-area relationships using radar rainfall data. *Journal of hydrologic Engineering* **7**(5): 356-367.

- Einfalt T, Nielsen KA, Golz C, Jensen NE, Quirmbac M, Vaes G, Vieux B. 2004. Towards a roadmap for use of radar rainfall data in urban drainage. *Journal of Hydrology* **299**: 186-202.
- EPA. 2004. Environmental Protection Agency. Multi-Resolution Land Characteristics Consortium - National Land Cover Data (NLCD) for Texas.
- Finnerty BD, Johnson D. 1997. Comparison of National Weather Service operational mean areal precipitation estimates derived from NEXRAD radar Vs. -raingauge networks. In *IAHR XXVII Congressional International Association of Hydraulic Research*, Delft, The Netherlands.
- Grecu M, Krajewski WF. 2000. Simulation study of the effects of model uncertainty in variational assimilation of radar data on rainfall forecasting. *Journal of Hydrology* **239**: 85-96.
- Griensven AV, Bauwens W. 2005. Application and evaluation of ESWAT on the Dender basin and the Wister Lake Basin. *Hydrological Processes* **19**: 827-838.
- Grimes DIF, Iguzquiza EP, Bonifacio R. 1999. Optimal areal rainfall estimation using raingauges and satellite data. *Journal of Hydrology* **222**: 93-108.
- Gupta HV, Sorooshian S, Yapo PO. 1999. Status of automatic calibration for hydrologic models: Comparison with multilevel expert calibration. *Journal of Hydrologic Engineering* **4**(2): 135-143.
- Jayakrishnan R. 2001. Effect of rainfall variability on hydrologic simulation using WSR-88D (NEXRAD) data. Ph.D. Dissertation submitted to Texas A&M University, College Station, TX.
- Jayakrishnan R, Srinivasan R, Arnold JG. 2004. Comparison of raingauge and WSR-88D Stage III precipitation data over the Texas-Gulf Basin. *Journal of Hydrology* **292**: 135-152.
- Johnson D, Smith M, Koren V, Finnerty B. 1999. Comparing mean areal precipitation estimates from RADAR and raingauge networks. *Journal of Hydrologic Engineering* **4**(2): 16451.
- Joss J, Lee R. 1995. The application of radar-gauge comparisons to operational precipitation profile corrections. *Journal of Applied Meteorology* **34**: 2612-2630.

- Koren VI, Finnerty BD, Schaake JC, Smith MB, Seo DJ, Duan, QY. 1999. Scale of dependencies of hydrologic models to spatial variability of precipitation. *Journal of Hydrology* **217**: 285-302.
- Krajewski WF, Smith JA. 2002. Radar hydrology: rainfall estimation. *Journal of Hydrology* **25**: 1387-1394.
- Kuczera G, Williams BJ. 1992. Effect of rainfall errors on accuracy of flood estimates. *Water Resources Research* **28**(4): 1145-1153.
- Masmoudi M, Habaieb H. 1993. The performance of some real time statistical flood forecasting models seen through multi criteria analysis. *Water Resources Management* **7**: 57-67.
- Neary VS, Habib E, Fleming M. 2004. Hydrological modeling with NEXRAD precipitation in Middle Tennessee. *Journal of Hydrologic Engineering* **9**(5): 339-349.
- Neitsch SL, Arnold JG, Kiniry JR, Williams JR, King KW. 2002. Soil and Water Assessment Tool Theoretical Documentation, 2000. Blackland Research Center, TAES, Temple, TX.
- Peschel JM, Haan PK, Lacey RE. 2003. A SSURGO pre-processing extension for the ArcView Soil and Water Assessment Tool, ASAE Annual International Meeting, Paper No. 032123, Las Vegas, NV.
- Peters JC, Easton DJ. 1996. Runoff simulation using radar rainfall data. *Water Resources Bulletin* **32**(4): 753-760.
- Racy JP, Kopsky ML. 1995. A comparison of NEXRAD precipitation estimates to Real-time data, Errata, *Central Regional Applied Research Papers* 15-06.
- Reed SM, Maidment DR. 1999. Coordinate transformations for using RADAR data in GIS-based Hydrologic modeling. *Journal of Hydraulic Engineering* **4**(2): 174-182.
- Serrano SE. 2004. Explicit solution to Green and Ampt infiltration equation. *Journal of Hydrologic Engineering* **6**(4): 336-340.
- Shah SMS, O'Connell PE, Hosking JRM. 1996. Modeling the effects of spatial variability in rainfall on catchments response. 1. Formulation and calibration of a stochastic rainfall field model. *Journal of Hydrology* **175**: 67-88.
- Smith JA, Seo DJ, Baeck ML, Hudlow MD. 1996. An Intercomparison study of NEXRAD precipitation estimates. *Water Resources Research* **32**(7): 2035-2045.

- SSURGO. 2005. Soil Survey Geographic database (SSURGO) for Texas, United States Department of Agriculture - Natural Resources Conservation Service.
- Stellman KM, Fuelberg HE, Garza R, Mullusky M. 2001. An examination of radar and raingauge-derived mean areal precipitation over Georgia watersheds. *Weather and Forecasting* **16**:133-144.
- Sun H, Cornish PS, Daniell TM. 2002. Spatial variability in hydrologic modeling using rainfall-runoff model and Digital Elevation Model. *Journal of Hydrologic Engineering* **7**(6): 404-412.
- Syed KH, Goodrich DC, Myers DE, Sorooshian S. 2003. Spatial characteristics of thunderstorm rainfall fields and their relation to runoff. *Journal of Hydrology* **271**: 1-21.
- Todini E. 2001. A Bayesian technique for conditioning radar precipitation estimates to rain-gauge measurements. *Hydrology and Earth System Sciences* **5**(2): 187-199.
- Tripathi MP, Panda RK, Raghywanshi NS. 2004. Development of effective management plan for critical subwatersheds using SWAT model. *Hydrological Processes* **19**: 809-826.
- Troutman BM. 1983. Runoff prediction errors and bias in parameters estimation induced by spatial variability of precipitation. *Water Resources Research* **19**(3): 791-810.
- Whiteaker TL, Robayo O, Maidment DR, Obenour D. 2006. From a NEXRAD rainfall map to a flood inundation map. *Journal of Hydrologic Engineering* **11**(1): 37-45.
- Winchell M, Gupta HV, Sorooshian S. 1998. On the simulation of infiltration- and saturation-excess runoff using radar-based rainfall estimates: effects of algorithm uncertainty and pixel aggregation. *Water Resources Research* **34**(10): 2655-2670.
- Vieux BE, Bedient PB. 1998. Estimation of rainfall for flood prediction from WSR-88D reflectivity: A case study, 18-18 October, 1994. *Journal of Weather and Forecasting* **13**(2): 407-415.
- Yang D, Goodison BE, Metcalfe JR, Golubev VS, Bates R, Pangburn T, Hanson CL. 1998: Accuracy of NWS 8" standard non-recording precipitation gauge: Result and application of WMO Intercomparison. *Journal of Atmospheric and Oceanic Technology* **15**: 54-68.
- Young RA, Allesi RS, Needham SE. 1992. Application of a distributed parameter model of watershed assessment. In *Managing water resources during*

*global change*. American Water Resources Association: Bethesda, MD.

Young CB, Nelson BR, Bradley AA, Smith JA, Peters-Lidard CD, Kruger A, Baeck ML. 1999. An evaluation of NEXRAD precipitation estimates in complex terrain. *Journal of Geophysical Research* **104**(D16): 19691-19703.

Zhang Z, Koren V, Smith M, Reed S, Wang D. 2004. Use of next generation weather radar data and basin disaggregation to improve continuous hydrograph simulations. *Journal of Hydrologic Engineering* **9**(2): 103-115.

## VITA

Name: Bakkiyalakshmi Palanisamy

Address: 1500, Research Parkway, Suite B223,  
2120 TAMU,  
College Station, TX 77843-2120.

Email Address: bakki\_23@tamu.edu

Education: B.E., Agricultural Engineering, Tamil Nadu Agricultural  
University, 2001  
M.S., Biological and Agricultural Engineering, Texas  
A&M University, 2006

Professional Experience: Engineering Associate, City of Austin, 2005-Present  
Executive Intern, South Dakota Department of  
Agriculture, 2005  
Graduate Research Assistant, 2002-2005  
Junior Research Fellow, 2002